CR 86083

TM-6-349-247

ELECTRON MICROSCOPE STUDY OF FILM NUCLEATION

BY K.J. KRONENBERG

FEBRUARY 1968

PREPARED UNDER CONTRACT NO. NAS 12-360 BY

GENERAL DYNAMICS, POMONA DIVISION

POMONA, CALIFORNIA

ELECTRONICS RESEARCH CENTER

NATIONAL AERONAUTICS AND SPACE ADMINISTRATION

TM-6-349-247

ELECTRON MICROSCOPE STUDY OF FILM NUCLEATION

BY K.J. KRONENBERG

FEBRUARY 1968

PREPARED UNDER CONTRACT NO. NAS 12-560 BY

GENERAL DYNAMICS, POMONA DIVISION

POMONA, CALIFORNIA

ELECTRONICS RESEARCH CENTER

NATIONAL AERONAUTICS AND SPACE ADMINISTRATION

TABLE OF CONTENTS

Summary

Introduction

Experiments

- The Equipment
- The Procedures
- Background Pressure at the Substrate and Contamination Problems
- Temperature Determination at the Substrate
- Deposition Rates

Results Obtained

- Iron Depositions at Various Temperatures
  - f.c.c. Iron Crystallites
  - b.c.c. Iron Deposits
  - Transformation from f.c.c. to b.c.c. Diffraction Rings
- Copper Deposition Above and Below 1/3 of Absolute Melting Temperature (AMT)
  - Copper Growth Under High-Purity Conditions
  - Copper Growth Under Room Temperature Conditions
- Gold Deposition at Room Temperature

Discussion of Results

- The Formation of Crystallites
- Liquid Phase
- Transformation of Crystal Lattice Type
- Change in Lattice Parameters
- The Growth Habit of b.c.c. Iron Particles
- Particle Growth and Environmental Conditions

References

LIST OF FIGURES

FIGURE

1. Substrate Inside Pt-Woven

2. Open Substrate

3. Cross Section Through In-Situ Deposition Equipment

4. Diffraction of Carbon Before Iron Deposition

5. Diffraction of Carbon After 3 Min. Deposition

6. Diffraction After 6 Min. Deposition

7. Diffraction After 15 Min. Deposition

8. Diffraction After 33 Min. Deposition

9. Image After 50 Min. Iron Deposition

10. Deposition Time in Minutes f.c.c. iron Deposition

11. Diffraction After 73 Min. Deposition

12. Diffraction of b.c.c. Iron Deposit

13. Image of b.c.c. iron deposit at room Temperature

14. Deposition Time in Minutes

15 Image of b.c.c. and f.c.c. Iron Mixed. Top Of Image Only f.c.c., bottom of image b.c.c. Diffr.

16. Diffraction of Iron Deposits During Transformation.

17. Diffraction of Iron After Transformation.

18. Image of Iron After Fast Deposition at Room Temperature

19. Deposition Time in Minutes.

20. Diffraction Before Start of Copper Deposition.

21. Diffraction After Start of Copper Deposition

22. Image of Carbon Before Start of Copper Deposition.

23. Image of Carbon After 3 Min. Copper Deposition

24. Diffraction after 3.5 Min. Copper Deposition

25. Image After 5 Min. Copper Deposition

26. Diffraction After 5.5 Min. Copper Deposition

27. Image After 7.5 Min. Copper Deposition

28. Image After 11 Min. Copper Deposition

29. Diffraction After 11.5 Min. Copper Deposition

30 Image 11.5 Min. After Start of Copper Deposition

31. Image 21.5 Min. After Start of Copper Deposition

32. Image 21.75 Min. After Start of Copper Deposition

33. Image 23.5 Min. After Start of Copper Deposition

34. Image 29.5 Min. After Start of Copper Deposition

35. Diffraction 19.5 Min. After Start of Copper Deposition

36. Diffraction 28 Min. After Start of Copper Deposition

37. Image of Globular Copper Particles Formed on Carbon After Cooling

38. Diffraction After Formation of Globular Copper Particles

39. Image of Copper Deposition, After 47 Min. at Room Temperature.

40. Image of Copper Deposition After 53 Min. at Room Temperature

41. Diffraction of Spherical Copper Particles

42. Image of Spherical Copper Particles at Room Temperature

43. Image of Gold Deposition After 9.5 Min.

44. Diffraction of Gold Deposition After 9 Min.

45. Image of Carbon After 16 Min. Gold Deposition

46. Image After 20 Min. Gold Deposition

47. Image after 33 Min. Gold Deposition

48. Image After 33 Min. Gold Deposition After Interruption for Change of Photographic Plates

49. Image After 33 Min. Gold Deposition After 1 Min. Exposure to Electron Beam

50. Image After 75 Min. Gold Deposition On Formerly Observed Location.

51. Image After 75 Min. Gold Deposition on Location Without Former Observation

52. Diffraction After 75 Min. Gold Deposition

SUMMARY

The formation of thin metal films has been observed by electron diffraction and electron microscopy during in-situ deposition on amorphous carbon films. Specifically, the formation of deposits of iron, copper and gold has been investigated at various temperatures for transformations of crystal structure, variations of atomic distances and phase changes (quasi liquid to solid) during early stages of growth. Whenever possible, such processes have been correlated to particle sizes.

The existence of crystallites with diameters of less than 20 Å was deduced from electron diffraction rings only. Particles with dimensions larger than 20 Å were observed directly from electron micrographs as well as by electron diffraction.

Structural transformations of the crystal lattice were only observed in deposits of iron. The initial deposits of iron maintained an f.c.c. structure until they grew to dimensions of approximately 50 Å. A transformation to a b.c.c. type crystal structure was then observed. No further change in structure occurred up to the formation of continuous iron film.

Unit cell dimensions in both types of iron crystals seemed to be largest in very small particles and decreased during the growth of crystallites. The f.c.c. crystal structure of iron particles between 20 and 50 Å size indicate a possible decrease in lattice parameters from 4.3 to 4.15 Å; however, measurement accuracy is too limited at such particle sizes to be certain. Somewhat more valid was the observation that b.c.c. iron crystals of about 50 Å size had lattice parameters of approximately 3.15 Å which decreased to 2.90 Å as the particles grew to be 100 Å and larger.

Copper and gold deposits started observable nucleation with an f.c.c. type lattice structure. The early deposits grew without any noticeable transformation in structure. No variation in lattice parameters could be noticed in the deposits of these two metals.

All deposits with dimensions of more than 80 Å showed well defined crystallization while diffraction patterns and images of smaller deposits indicated incomplete crystallization. No "liquid" phase was found at any stage of the metal deposits. Various shapes of crystallites were found and described.

The observations of the in-situ depositions performed under this four month's contract are summarized in Table I.

TABLE I

Deposited Material	Deposition Temperature (nominal only !)	Particle Size of f.c.c. type crystallites (Å)	Particle Size of b.c.c. type crystallites (Å)	Changes of lattice parameters (Å)	Smallest size of apparently fully crystalline deposits (Å)	Liquid phase
Iron	Room temp.	10-30				not observed
	300°C	10-50		(4.3 to 4.15, uncertain)		not observed
	500°C	10-50		(4.2 to 4.15, uncertain)		not observed
	300°C		> 50	3.15 - 2.90	80-90	not observed
	500°C		> 50	3.10 - 2.90	80-90	Not observed
Copper	room temp.	10-80	none observed	3.62 no change observed	80	not observed
	above 1/3 melting temp.	10-80	none observed	3.62 no change observed	80	perhaps surface layers
Gold	room temp.	5-80	none observed	4.08 no change observed	80	not observed

INTRODUCTION

In-situ electron microscope observations of thin film formation during the deposition process have a decisive advantage when compared to studies of deposits which have been produced in another vacuum system. The interruption of the deposition and the transfer into the observation system may cause considerable changes of the deposit before it can be studied. (Ref. 1, 2, 3). Since the first experiments with in-situ thin film deposition by McLauchlan (Ref. 4, 1950) attempts have been made to overcome the difficulties inherent in such observation (Ref. 5 - 14). In most commercial electron microscopes space for experimentation is very limited, particularly in the vicinity of the object under observation. The operational vacuum of most instruments is inferior to most thin-film deposition requirements. The electron beam necessary for the observation can have a significant influence on the deposition itself and on the deposited material.

The four-month effort, reported in the following, was based on equipment formerly described by H. Poppa (Ref. 14) which is attached to a commercial electron microscope (Hitachi 11A). This equipment represents notable improvements relative to that used by earlier investigators mainly pertaining to control of environmental conditions at the site of deposition. Some further improvements of controlled environment has been achieved during the course of this work by additional pumping capability and by implementing temperature measurements at the substrate holder.

The observations reported here should be considered exploratory in nature. Quantitative analysis and conclusions of a more general nature should be attempted only after verification by repeated experiments under reproducible conditions.

EXPERIMENTS

The Equipment

The holder for the carbon film substrates (Figures 1 and 2) was a platinum sheet with 85-μ holes which could be heated up to 800 degrees centrigrade. It was closely encapsulated by a cartridge which was connected to a liquid nitrogen reservoir by thermal conductors. A platinum-platinum rhodium thermocouple was attached inside the heating oven or in case of direct heating to the platinum sheet. A temperature gradient of several hundred degrees per MM was maintained constant for the duration of every experiment in the immediate vicinity of the substrate to facilitate cryogenic pumping of the sample environment. The substrate was penetrated perpendicularly by the observation beam of the electron microscope.

The beam of the evaporated metal fell on the heated substrate at an angle of about 55°. (Figure 3). The vapor beam travelled through cooled tubes after leaving either of two source heaters. The latter consisted of shielded tungsten wire baskets with a conical opening toward the substrate. Each basket was heated by a stabilized d.c. current from a battery. The metal to be evaporated was melted onto the wire of the basket. A water cooled crystal oscillator could be moved to intercept the vapor beam about halfway between source and target. It served as a shutter and as monitor for establishing and controlling a constant evaporation rate. The two source ovens could be operated independently of each other and their vapor beams could be exchanged within a second. The principal purpose for having two sources was to provide a means for starting metal evaporations on a freshly deposited substrate surface (amorphous carbon).

The deposition system, consisting of the substrate heater-holder and the evaporator, was placed into the Hitachi 11A electron microscope in the position normally occupied by the object holder (utilizing the modified pole piece for the object heater), and the standard object changer. The electron microscope was operated with three diffusion pumps. This provided additional pumping power relative to the normal operation with two standard diffusion pumps. A calibrated vacuum gauge monitors the background pressure in the microscope columns.

The Procedures

Carbon films of about 200 - 300 Å thickness were vacuum deposited on Victawet covered glass sides in a vacuum system at about 10^{-6} torr background pressure. Immediately afterwards, chips or granules of the source material, metals of 99.999% purity, were melted on the wire of the heater basket in the same vacuum system. By appropriate arrangement of

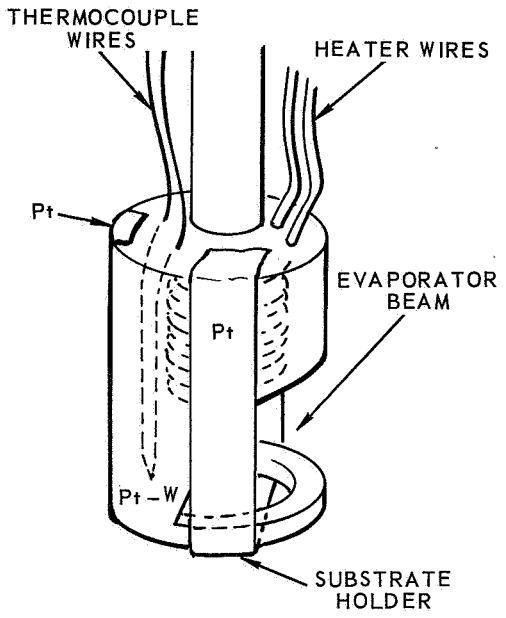

Figure 1. Substrate Inside Pt-W Oven.

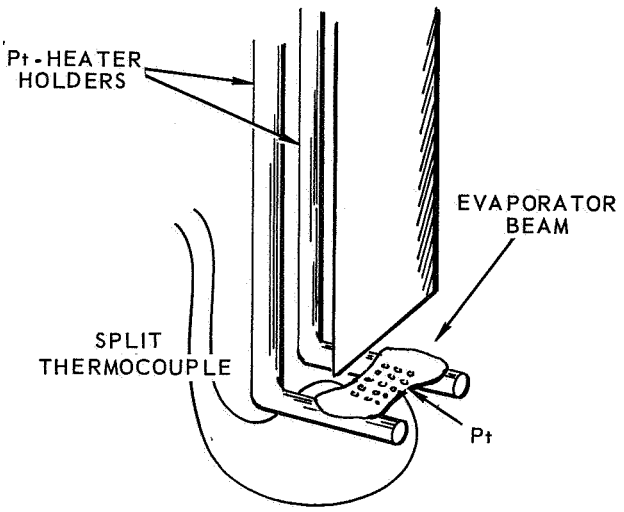

Figure 2. Open Substrate.

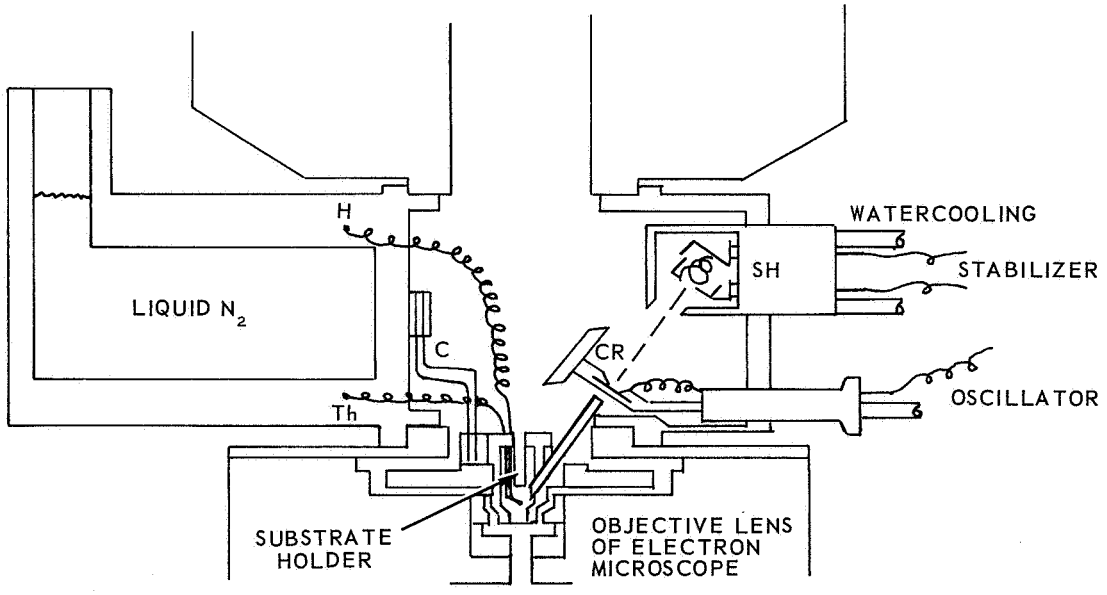

H = HEATER TERMINAL FOR SUBSTRATE; C = COOLING CONDUCTOR
TH = THERMOCOUPLE TERMINAL; CR = CRYSTAL MONITOR – SHUTTER
SH = SOURCE HEATER ARRANGEMENT

Figure 3. Cross Section Through In Situ Deposition Equipment.

the slides, clean carbon films were obtained as well as carbon films with various amounts of deposited source material. The latter were used, in several cases, for comparison with the in-situ formed deposits.

Parts of the pure carbon films were floated off and placed on the flame cleaned platinum substrate holder. Then substrate and source oven were installed and pumped under mild heating. The suitability of the substrate was tested by electron diffraction and electron micrographs. and potential observation areas were selected. Cooling of the system by liquid nitrogen and the heating of the substrate for the desired deposition temperature were started. Before initiation of deposition, temperature stabilization was established which required time periods of up to several hours.

Only minutes were required to establish a constant evaporation rate. Very slow rates were selected which permitted extended observation times of initial nucleation. For studies of growth and phase transformations, higher evaporation rates were used which produced substantial coverage of the substrate within about 30 minutes.

Background Pressure at the Substrate and Contamination Problems

Prior to experiments in our microscope system, the background pressure of the in-situ evaporator unit had been measured in an equivalent microscope by Poppa (Ref. 13), using the substrate holder inside the magnetic field of the objective lens as an electrode of a discharge gauge. The calibration with a commercial ion gauge was only possible without the cooling cartridge around the substrate holder. Poppa found a linear relationship between the discharge current and the pressure down to 10^{-6} torr. With the cooling cartridge in place, the discharge current indicated a pressure at the substrate holder of 5×10^{-8} torr under the assumption of extended linearity.

Order of magnitude confirmation was derived independently by Poppa from observations of the effects which the electron beam exerts on substrates before and after a layer of adsorbed gases has formed. A freshly prepared and outgassed substrate did not show any differences of nucleation processes between areas which were under the influence of the observing electron beam and such areas which had not been under this influence. Under common operational pressures in the electron microscope (in Poppa's system about 5×10^{-5} torr) it takes only a few seconds of film ageing until a change in appearance of the substrate can be observed in any area which is moved into the observation beam. The causes for the changes in film appearance under the influence of the electron beam are complex. Desorption of adsorbed gases causes some of the common observations as do differences in nucleation rates and growth habits. The time which elapses until a clean substrate starts to show differences between areas under extended observation and areas just

moved into the observation beam can be taken as an indicator for the effective prevention of contamination. Poppa (Ref. 14) in his cryogenically pumped system observed no beam influence on new substrates for 120 seconds in qualitative agreement with the local pressure values indicated above.

Our arrangement used the identical unit for the substrate space. The instrument background pressure and pump speed however, was improved by use of the third diffusion pump (to less than 2×10^{-5} torr). Heating of the platinum substrate to 500°C without liquid nitrogen cooling gave no beam effect on the substrate appearance for nearly 3 minutes. With liquid nitrogen cooling, observation times up to 20 or 30 minutes were required until differences between areas under continuous observation and other areas could be observed. While these observations are quite qualitative, indications are that the environment used in this program was as good or better as was utilized by Poppa during earlier work.

The source material was used in form of turnings which were produced with new cutting tools from metal slugs of 99.999 purity only a few hours prior to the melting onto the tungsten wire baskets. The evaporation beams traveled through water-cooled and liquid-nitrogen cooled tubes from the shielded source heater to the substrate. The mass flow rate of the vapor varied with the material and the source heater current which was (between 2.4 amp and 5.0 amp) adjusted in every case for the desired evaporation rate. Such an arrangement is favorable for maintaining an uncontaminated vapor beam, since the cooled tubes will reduce considerable background contamination in the beam itself.

Temperature Determination at the Substrate

The low temperature experiments reported here was principally performed by heating of the platinum substrate holder in an oven (designed for magnetic investigations) with a built-in thermocouple close to the platinum substrate holder (Figure 1). The oven was heated to the desired temperature (300°C or room temperature) and held constant by slight adjustments of the heater current. The closed form of the oven, however, did not promote the cryogenic purification of the substrate surface as well as does the open form (Figure 2) used for the higher temperature experiments.

The open form, however, made temperature determinations more difficult. The mean distance between parts of the cooled encapsulation and the direct heated platinum sheet was about one to two millimeter. At higher temperatures, the temperature gradient in this space is several 100°C per millimeter. Any conductive protrusion from the platinum sheet into this space reaches decisively closer to a cooled surface and represents a heat sink. To overcome some of the inherent problems, several improvements were developed during this contract.

Instead of a normal, one point thermocouple junction of platinum-platinum rhodium, the platinum leg and the platinum rhodium leg are mounted separately to the substrate holder to minimize the local heat sink. The thermovoltages are measured by using a calibrated high speed recorder during short interruptions of the heater current. This elimiates the effect of the direct heater current on the split thermocouple. The rapid cooling effect on current turn-off is accounted for by extrapolation of the emf curve to zero time, i.e., the instant of current turn-off. The method was validated by simultaneous thermocouple and pyrometric measurements. Correlatability was established to within at least the limit of the pyrometer accuracy.

The temperature of the deposit under observation differs, of course, from the temperature of the substrate holders to the degree controlled by the heat conductivity of the deposit material. This is a problem to all deposition techniques and cannot be fully eliminated. Any analysis or the specification of any experimental conditions must therefore, be performed with the substrate surface temperature as the reference temperature.

Deposition Rates

In the available system, a crystal oscillator intercepts the evaporation beam before and after each deposition experiment. In this manner the evaporation rate can be monitored as to consistency during the experiment. However, the different sticking coefficients of materials at different temperatures, etc., prevent reliable correlation between the deposition rates at the oscillating crystal and at the substrates. Nor does it permit the control or quantitative measurement of a given deposition rate.

After completion of every experiment, an attempt has been made to observe interferometrically the thicknesses of the entire assembly of substrate film and deposit and of carbon film which had not been hit by the source material. However, an interpolation for various stages of growth was not attempted. The deposition rates for the early nucleation stages, on the empty carbon, are likely to be quite different from the deposition rates during later stages of growth.

Our observations did not include continuous films for which thickness is a meaningful parameter. During any state of nucleation, a thickness equivalent in form of mass per unit area can only be estimated from the number of particles found per unit area and their sizes. However, to get the thickness information, profiles of single deposited particles would have to be measured. This can only be done at such locations where the carbon substrate, after deposition, has split and curled, exposing the deposit in profile. Though such locations have been found, no systematic effort was made in this matter as yet.

Thickness determination or mass measurement by inelastic scattering of electrons combined with quantitative photographic density evaluation (References 15, 16) is being contemplated for future work but has not been attempted in this contract period.

RESULTS OBTAINED

Iron Depositions at Various Temperatures

f.c.c. Iron Crystallites. - In every in-situ deposition experiment the first evidence of a deposition taking place on the carbon substrate was the appearance of one diffuse diffraction ring. In case of iron, this ring became visible inside the innermost diffraction ring which originated from the amorphous carbon. (Figures 4 and 5). With further deposition, more diffraction rings appeared with larger diameters (Figures 6, 7 and 8). They were measured as they became successively sharper and could be indexed as (111), (200) and (220). Assuming their origin to be f.c.c. type crystallites, the ring diameters indicated a lattice parameter of 4.2 ± 0.3. A more accurate determination was not possible because the rings of this system never lost their diffuse character.

At this state of the deposition, the contrasts in electron images were very low. Particle contours could not be recognized. A granulation of dimensions from 20 to 40 Å was observed by a through-focus series of high enlarged images in order to eliminate possible artifacts due to imperfect focusing or due to the photographic grain. The granulation seemed to cover the carbon substrate without any prevailing order or direction (Figure 9).

An iron deposition in this situation could be considered as consisting of some amorphous material between a large number of very small crystallites with an f.c.c. crystal lattice. The existence of only a few low-index diffraction rings of diffuse character indicates crystallites consisting of a few cells only (Ref. 17).

Changes of the diameters of the diffraction rings were within the range of inaccuracy. However, measurements of diffraction rings at early stages of nucleation particularly from the innermost ring alone - tended to place the intensity maximum at a smaller diameter than at later state of deposition (Figure 10). This was consistent and points toward a larger cell size for smaller nuclei and a cell size shrinking with growing numbers of atoms participating in the formation of the crystallites. The largest f.c.c. crystallites in our samples had lattice parameters between 4.15 Å and 4.2 Å, the smallest nuclei with identifiable crystal lattice showed lattice parameters between 4.2 and 4.3 Å.

b.c.c. Iron Deposits. - Iron deposits which were permitted to grow to particles sizes of 100 Å or more always consisted of crystallites with a b.c.c.-type lattice and a lattice parameter of approximately 2.90 A (Figures 11 and 12). However, the shape of these crystallites was not as observed in other metal films. Only few crystallites existed which gave the appearance of being nearly cubic in shape. Most of the

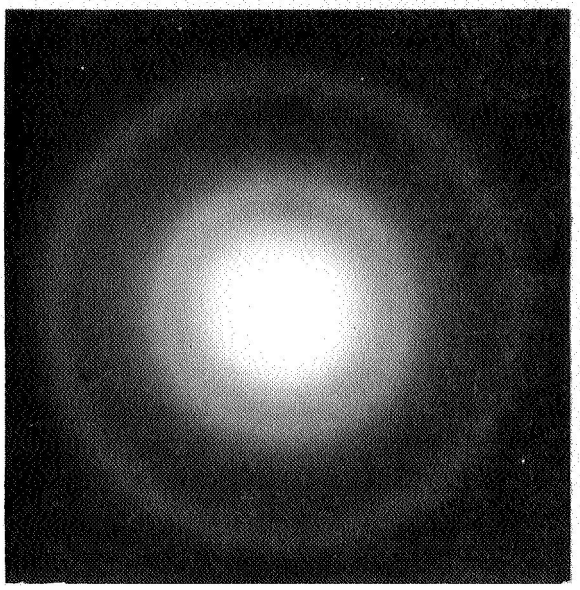

Figure 4. Diffraction of Carbon Before Iron Deposition.

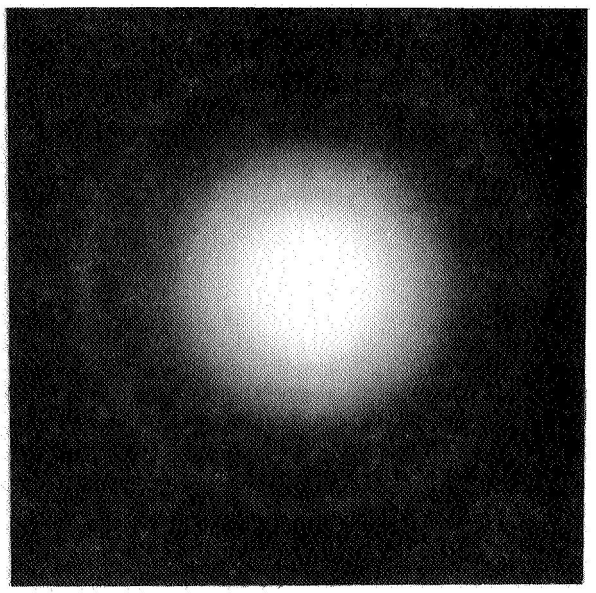

Figure 5. Diffraction After 3 Minutes Deposition.

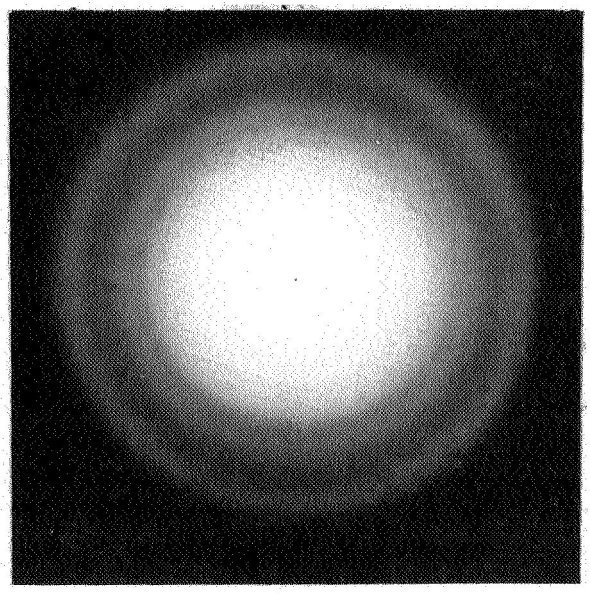

Figure 6. Diffraction After 6 Minutes Deposition.

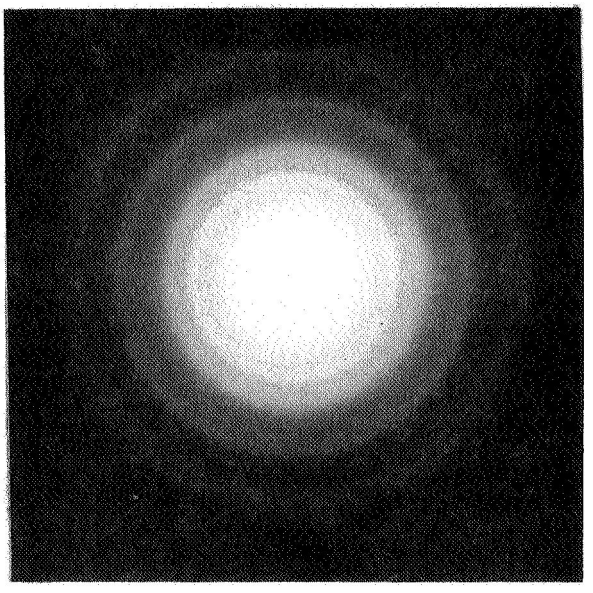

Figure 7. Diffraction After 15 Minutes Deposition.

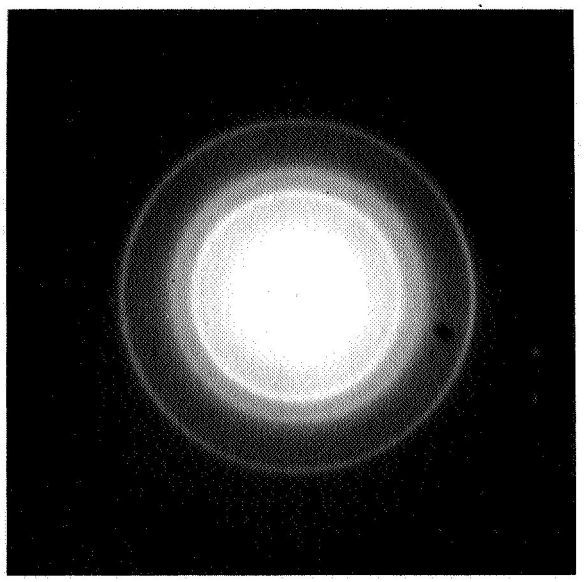

Figure 8. Diffraction After 33 Minute Deposition.

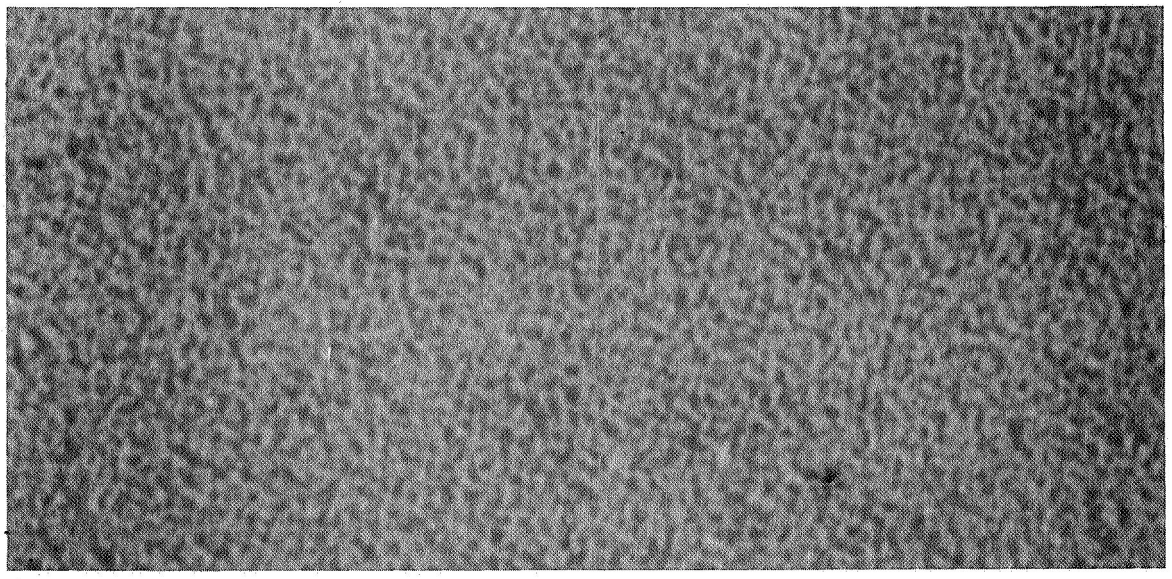

Figure 9. Image After 50 Minute Iron Deposition, no b.c.c. Iron in Evidence, Magnification 1 : 435,000.

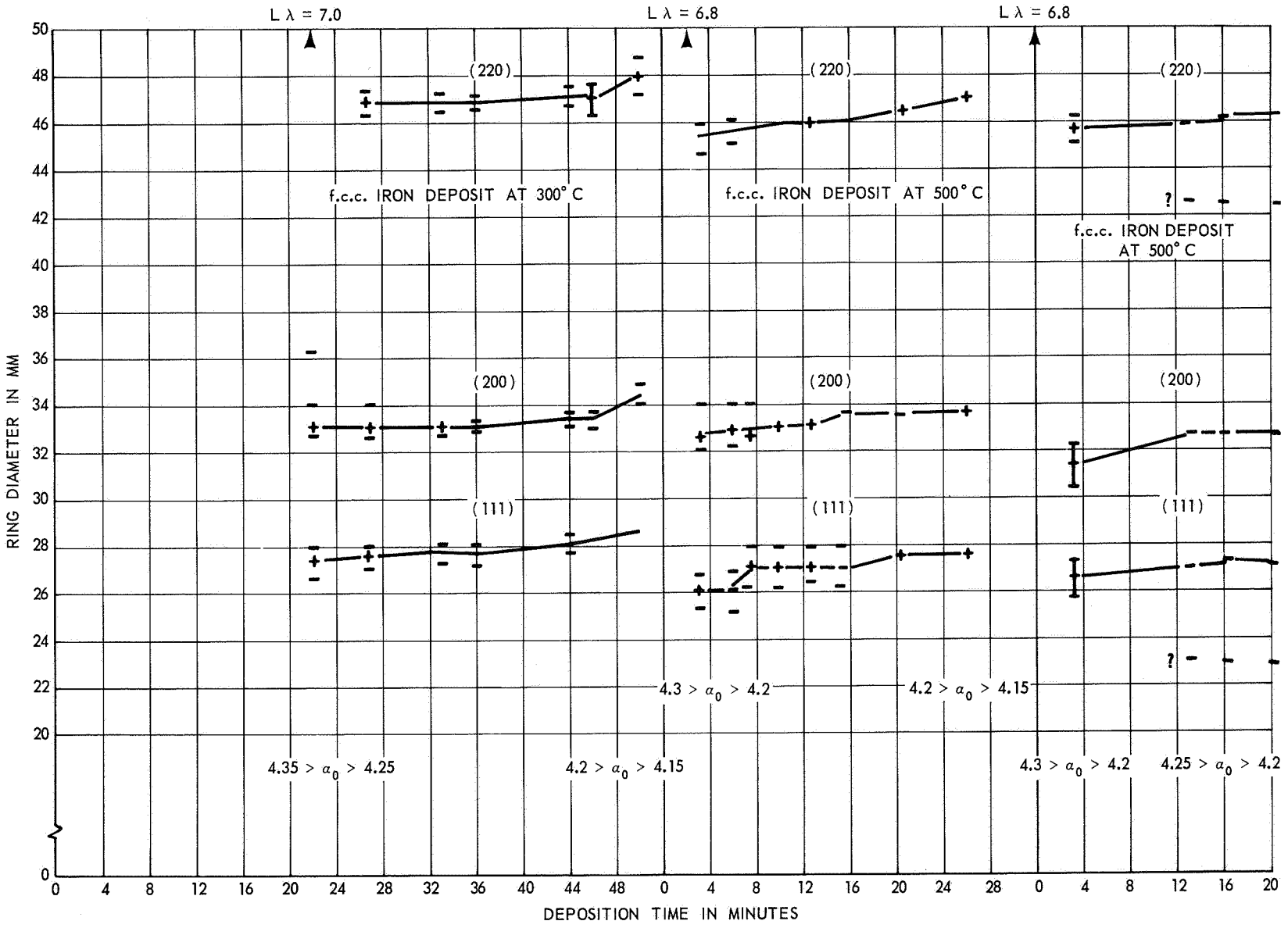

Figure 10. Deposition Time in Minutes f.c.c. Iron Deposition.

area of these films was covered by regions with a pronounced substructure (Figure 13). Such regions usually extended over 200 to 300 Å and were filled with a network of elongated particles parallel to each other. Two preferred directions, approximately perpendicular to each other, were noted. The thickness of the elongated crystallites was seldom more than 30 Å and the distances between them were 30 to 50 Å. Their length was usually 200 to 300 Å and occassionally up to 500 Å. This film structure was observed on iron films made with a sufficiently high evaporation rate under pure conditions (pure carbon substrate, pure iron source, good cryogenic vacuum environment).

Interesting as this habit of iron growth may be, possibly in connection with effects of spontaneous magnetization on nucleation and growth, the appearance of these deposits made it impossible to define a particle size. The thickness of such layers was determined by interferometer to be about 250 $\pm$ 50 Å.

Diffraction ring systems which suggested b.c.c. indexing developed in the form of well defined rings. Their diameters increased with further growth of the deposits. The first ring systems identifiable as b.c.c. (see next paragraph) were measured to have lattice parameters of 3.15 Å. The cell length became successively smaller and reached a final value of about 2.90 Å for all deposits which exhibited the structure described in the preceding paragraph (Figure 14).

Transformation from f.c.c. to b.c.c. Diffraction Rings. - During in-situ deposition observations of iron at elevated temperatures, the co-existence of f.c.c. type and b.c.c. type crystallites was evident from diffraction patterns of adjacent areas. Figure 15 shows the image of a deposit which consists in one corner of f.c.c. type, at the opposite side of b.c.c.-type material. In some areas diffraction patterns appeared, which could be described as a diffraction originating from a b.c.c.-type crystal with a distortion. A number of lines appeared to be split (Figure 16). These rings had diameters which could be indexed as (311), (222) and (331), (420), respectively in the f.c.c. system. At the location of these ring pairs, the split (211) and (310) rings of the b.c.c. diffraction were found. After several minutes of continued deposition the diffraction rings showed an undistorted b.c.c. lattice (Figure 17).

At the time of transformation, particles were visible in the images of the deposits. They had no sharp contours but they had dimensions of 40 to 50 Å. Particles larger than 50 Å were b.c.c. crystallites and assumed elongated shapes when growing.

At no time during the deposition and at no temperature from room temperature to about 500°C did we observe phenomena which could indicate a liquid-type behavior or part-liquid crystals. The contours were always undefined, but, any form of cofluence or coagulation was not

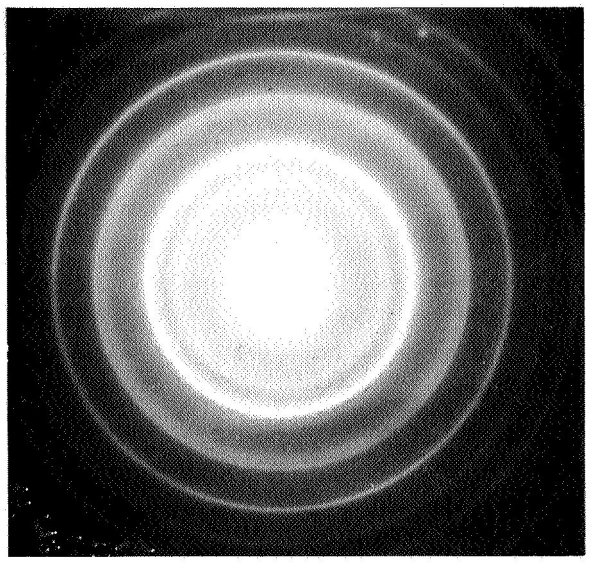

Figure 11. Diffraction After 73 Minute Deposition.

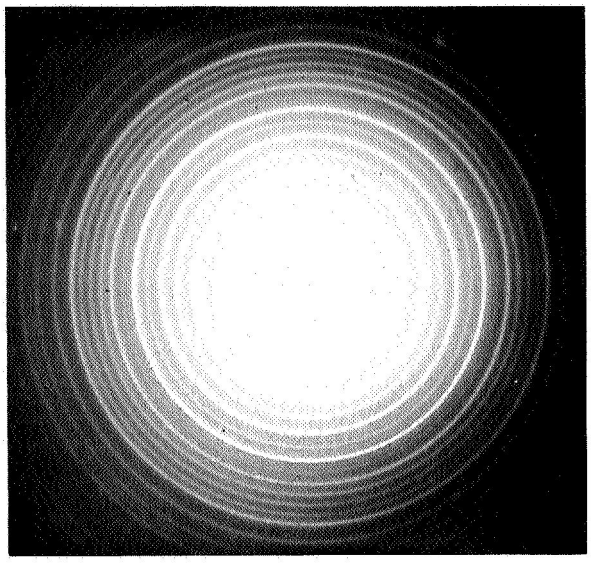

Figure 12. Diffraction of b.c.c. Iron Deposit.

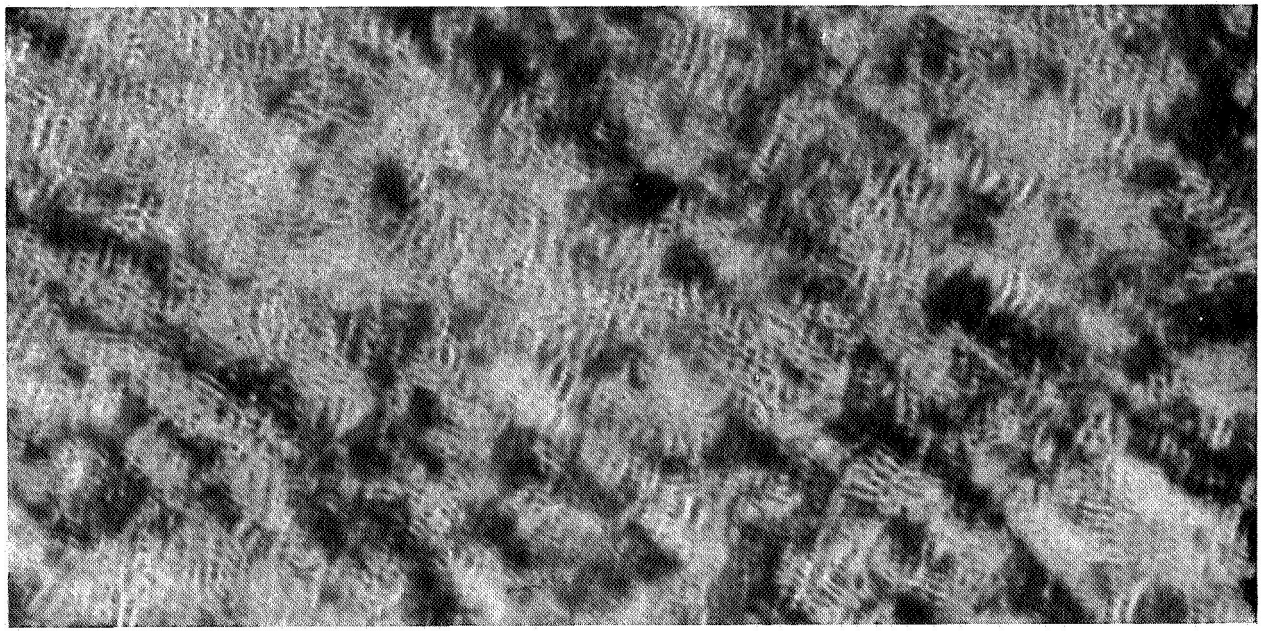

Figure 13. Image of b.c.c. Iron Deposit at Room Temperature, Magnification 1: 296,000.

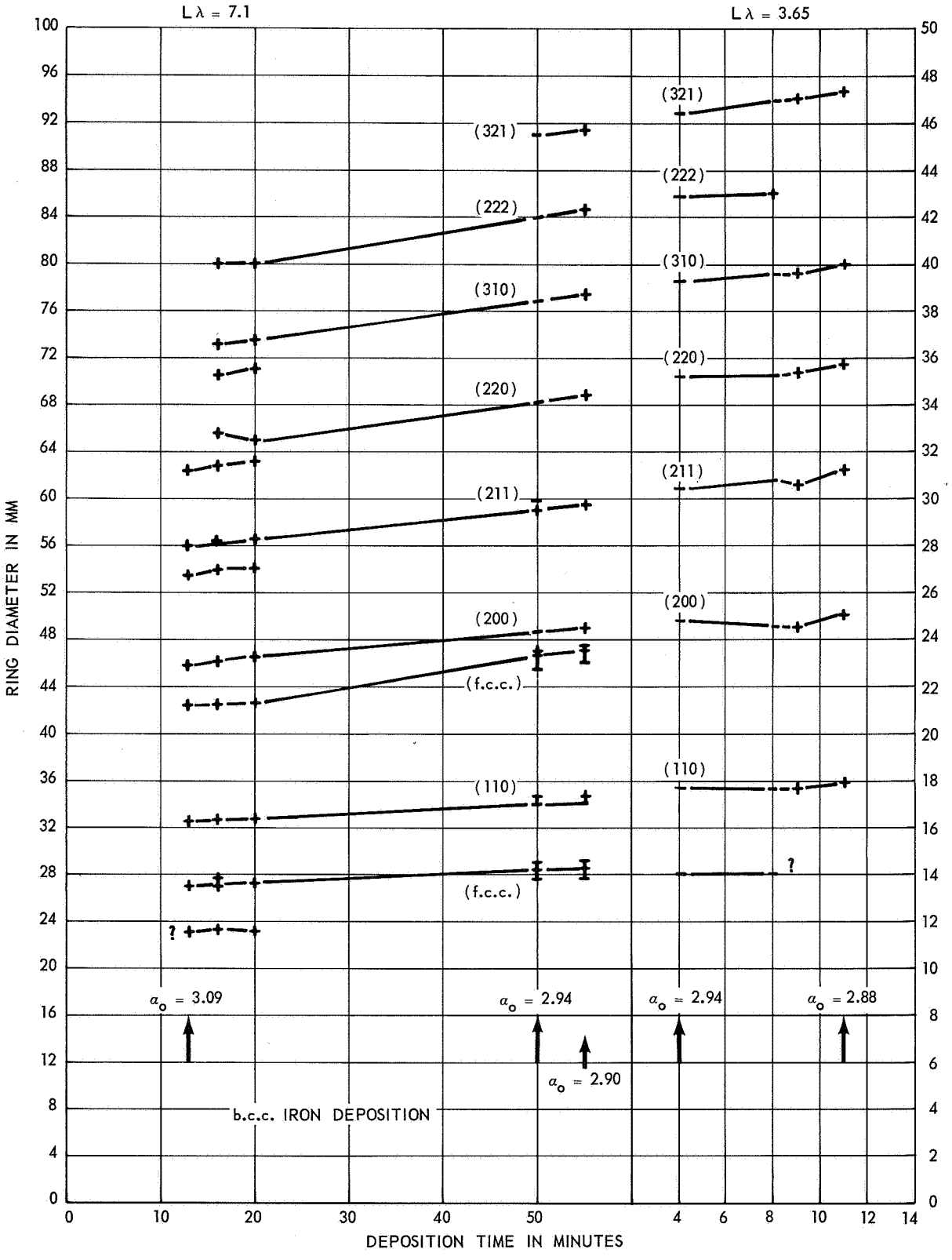

Figure 14. Deposition Time in Minutes.

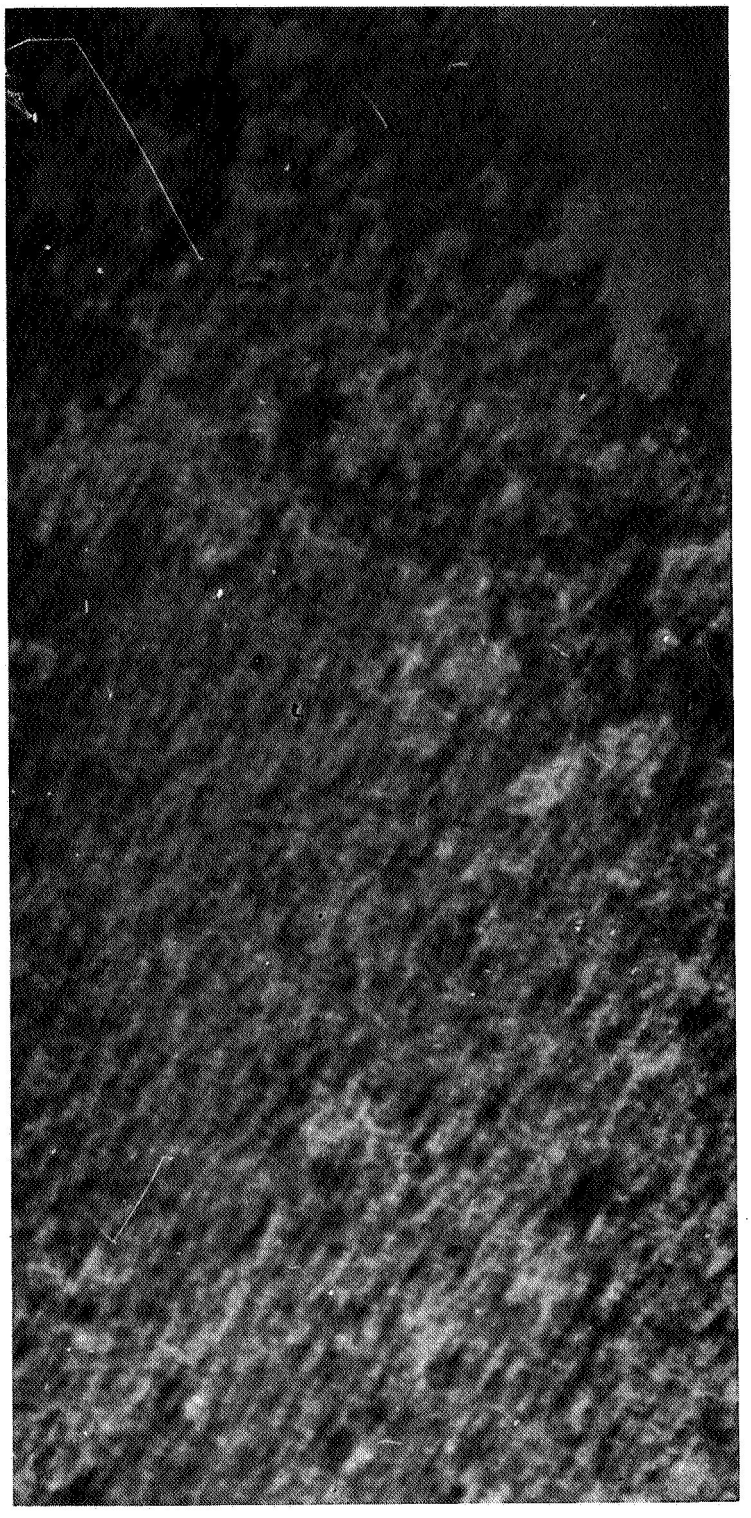

Figure 15. Image of b.c.c. and f.c.c. Iron Mixed. Top of Image Only f.c.c., Bottom of Image b.c.c. Magnification 1 : 200,000.

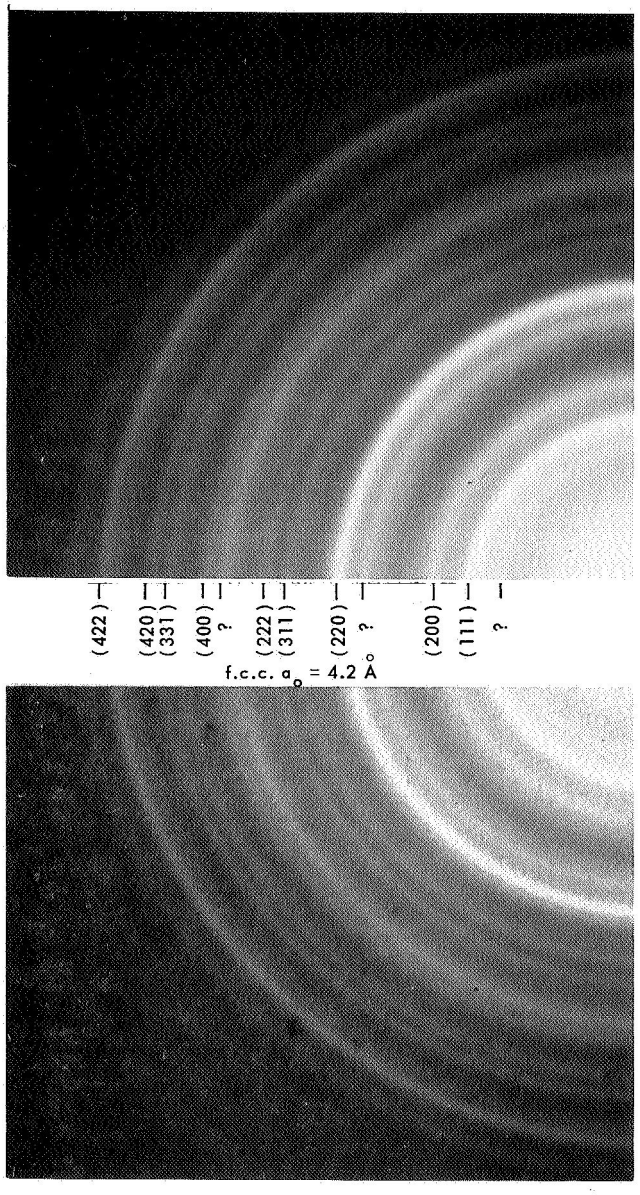

Figure 16. Diffraction of Iron Deposited During Transformation.

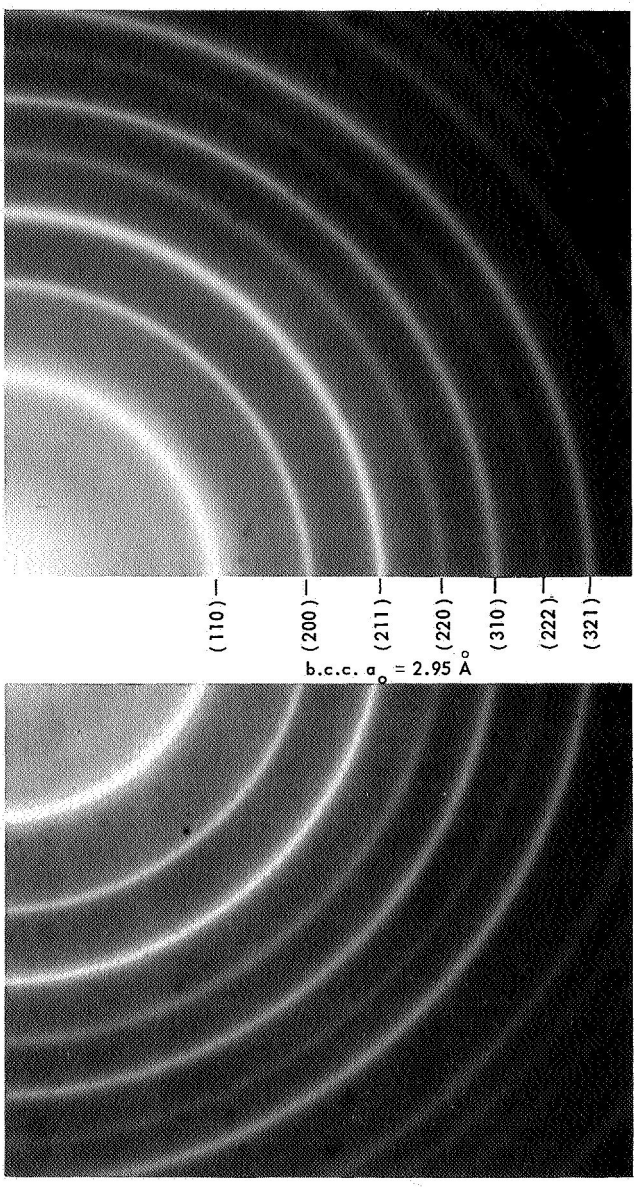

Figure 17. Diffraction of Iron After Transformation.

observed. A pronounced tendency of b.c.c. crystallites to align in straight rows was observed in most deposits of b.c.c. structure. This however, did not result in visible coagulation.

Fast depositions of iron at room temperature with less controlled purity conditions formed layers which seemed to consist of coagulated particles. However, high resolving electron images revealed these "particles" to have extremely complex substructures often with detail dimensions of less than 10 Å (Figure 18).

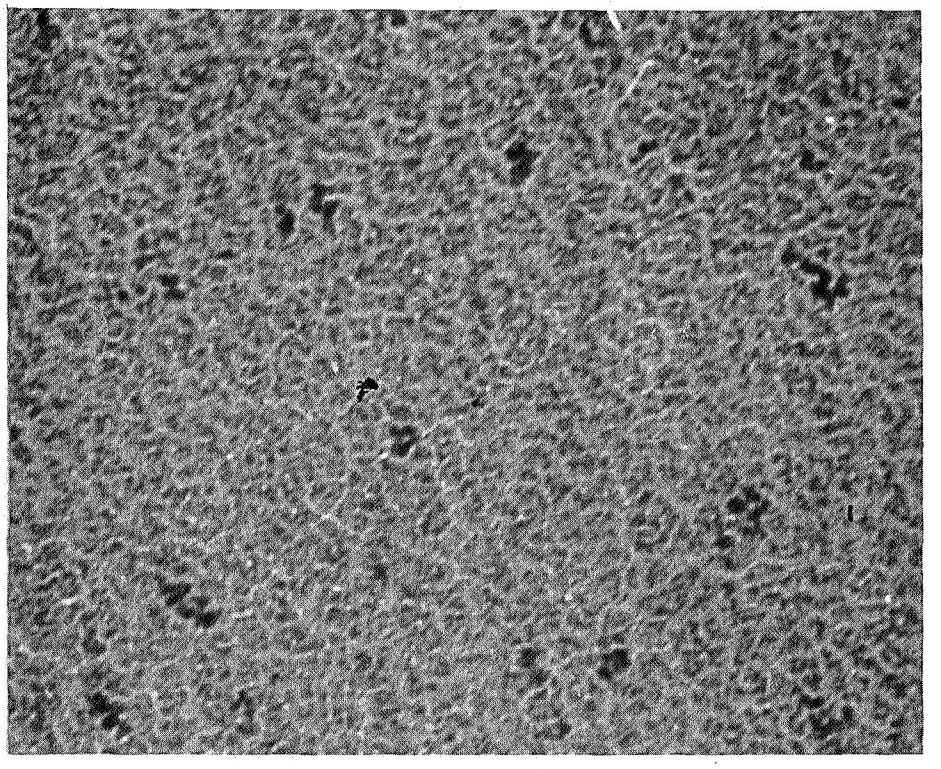

Figure 18. Image of Iron After Fast Deposition at Room Temperature, Magnification 1 : 435,000.

Copper Deposition Above and Below 1/3 of Absolute Melting Temperature (AMT)

Depositions of copper was observed, in-situ, on carbon substrates heated to room temperature and to a nominal value of 400°C. The latter temperature is about halfway between 1/3 and 2/3 of the absolute melting temperature (1356°K) or copper. (1/3 AMT = 452°K = 179°C; 2/3 AMT = 904°K = 631°C). Every observation made on copper depositions, independent of the temperature applied, showed crystallites of an f.c.c. lattice type with a cell edge distance of 3.62 ± 0.01 Å. Variations of the lattice parameters were uncorrelated to length of deposition time or particle size even for copper nuclei which were too small to produce more than the innermost (111)-ring of the f.c.c. diffraction pattern. (Figures 19 and 21). No liquid phase could be identified. With the questions about any transformation answered in the negative, the in-situ observed deposition of copper can be evaluated only with regard to deposition and growth phenomena.

Copper Growth Under High-Purity Conditions. - Evidence for copper deposition started with the appearance of the innermost ring (111) of it's f.c.c. diffraction pattern just inside of the first diffuse ring from the amorphous carbon substrate (Figures 20, 21). Simultaneously, a deepening in contrast had occurred in the image of the carbon substrate which displayed, when still empty, a slightly oriented corrugation (Figures 22, 23). The image in Figure 23 has the appearance of a carbon film after shadow casting. The deposition does not show a granulation of its own within the resolving power of the microscope. Particles of 15 A could have been detected with certainty if they existed.

The appearance of only the lowest index diffraction ring, in Figure 21, taken prior to image in Figure 23, indicates that the initial nucleated crystallites are composed of little more than one cell of the f.c.c. lattice. While, after the appearance of the image feature in Figures 22, the deposit produced the 4 lowest-indexed diffraction rings (Figure 24). This indicated crystallites to be composed of at least 365 atoms or about 64 cells (Ref. 17). The average size of such a crystallite would be about 4 times the cubic lattice parameter, i.e., in the case of copper, about 14 Å - just above the resolving power of the microscope.

The next image (Figure 25) of this deposition was taken about 90 seconds later. By then a significant change in the deposition mechanism had taken place. Many particles could be seen that had grown to about 50 A diameter. Diffraction rings with higher indices were visible (Figure 26). Though details of the contours were not resolved, these particles were usually surrounded by a white zone of empty carbon. These zones varied in width between 50 and 80 Å. Continued deposition resulted in further growth of the visible particles (Figures 27, 28). The general arrangement of the particles was maintained. The space

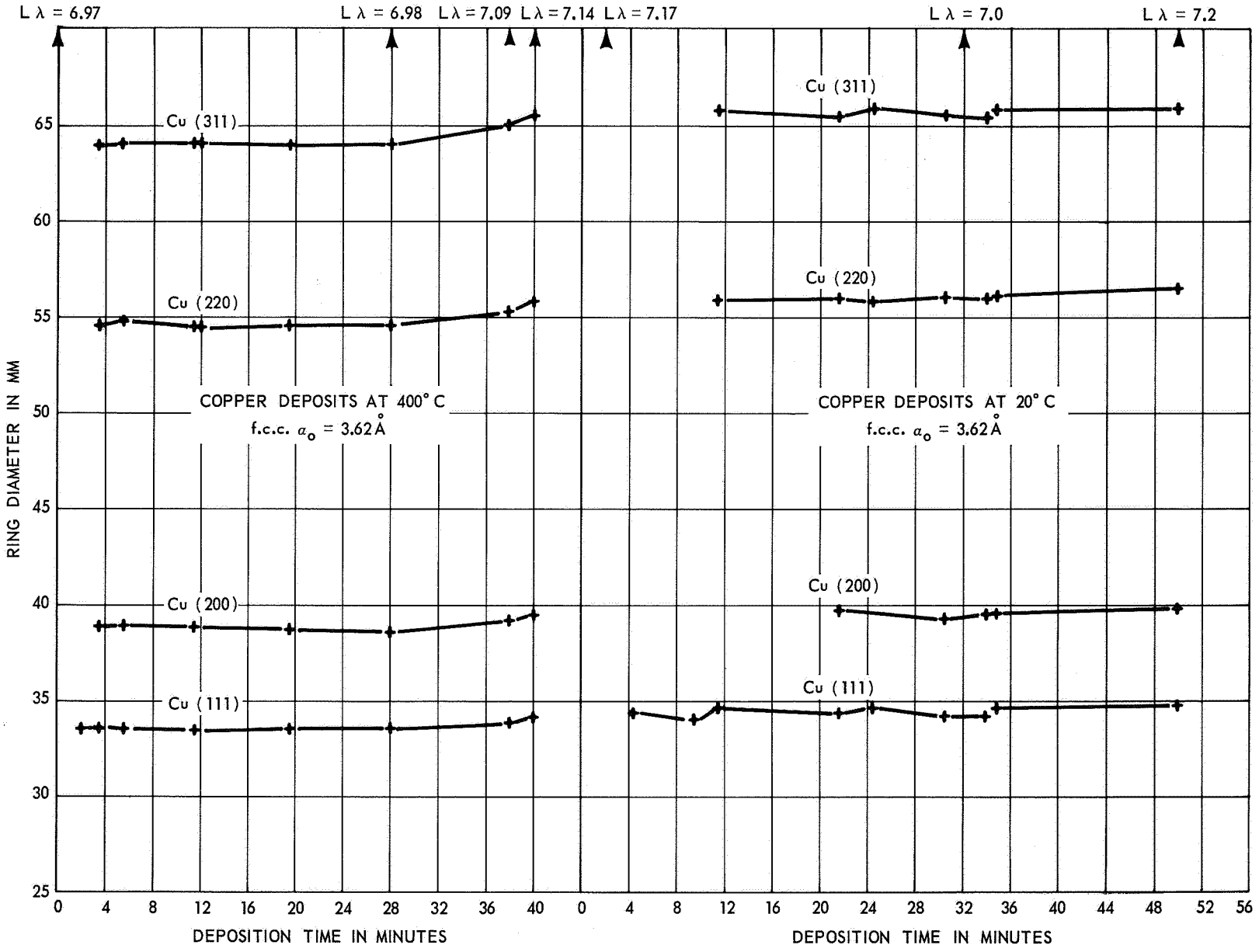

Figure 19. Deposition Time in Minutes.

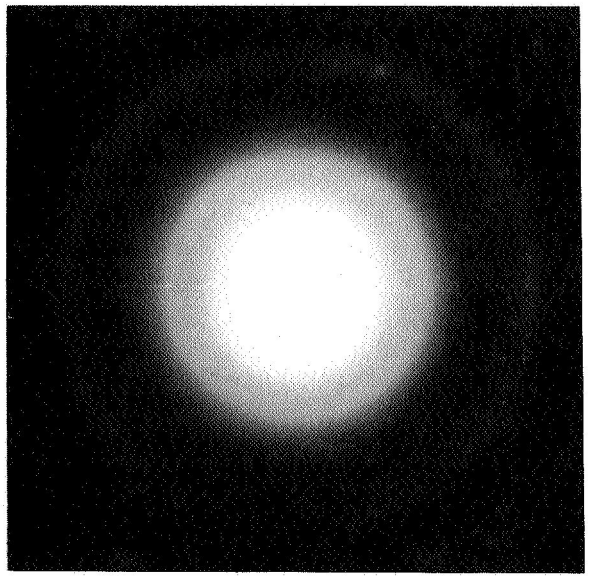

Figure 20. Diffraction Before Start of Copper Deposition (Image Figure 22).

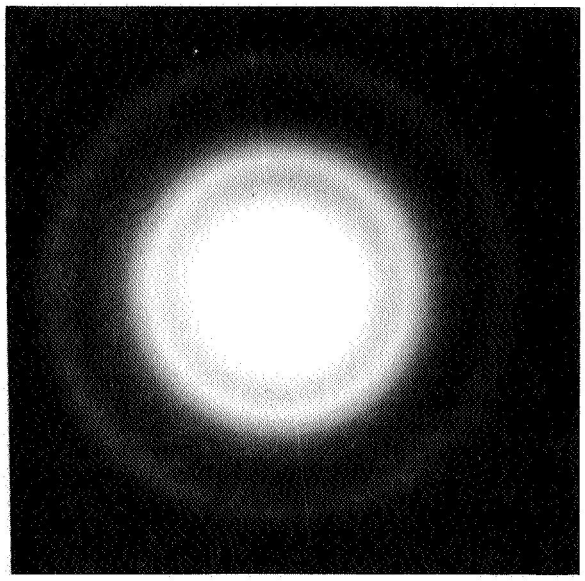

Figure 21. Diffraction After Start of Deposition.

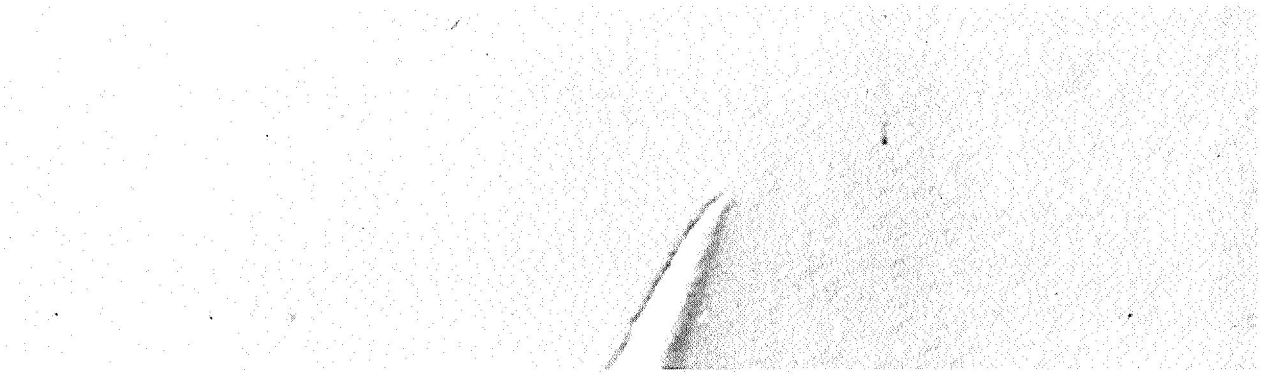

Figure 22. Image of Carbon Before Start of Copper Deposition (Diffraction Figure 20) Magnification 1 : 120,000.

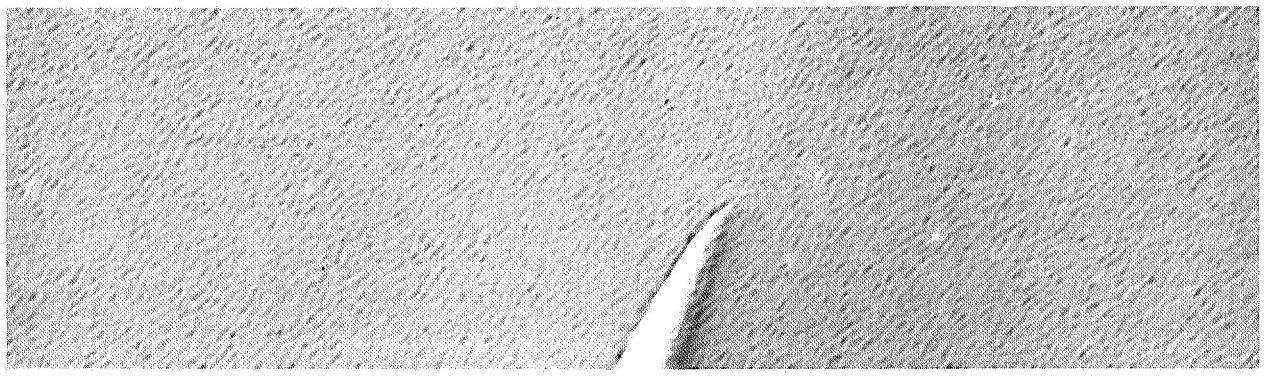

Figure 23. Image of Carbon After 3 Minute Copper Deposition (Diffraction Figure 24) Magnification 1 : 120,000.

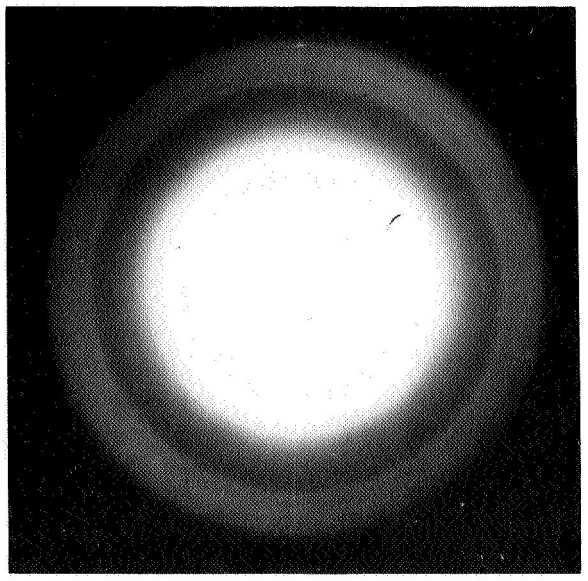

Figure 24. Diffraction After 3.5 Minute Deposition (Image Figure 23).

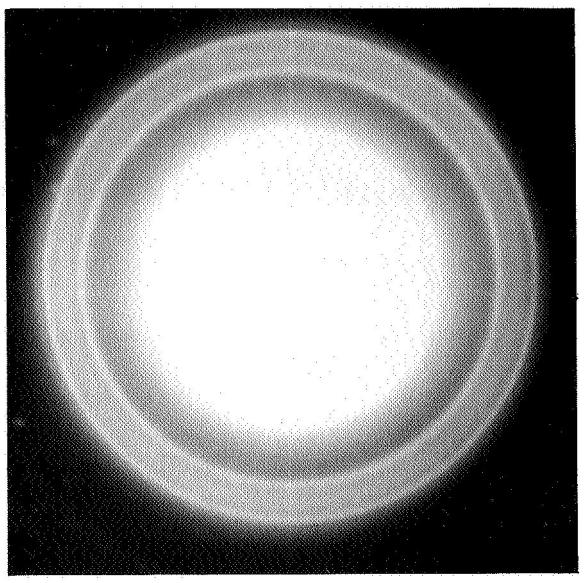

Figure 26. Diffraction After 5.5 Minute Deposition (Image Figure 25).

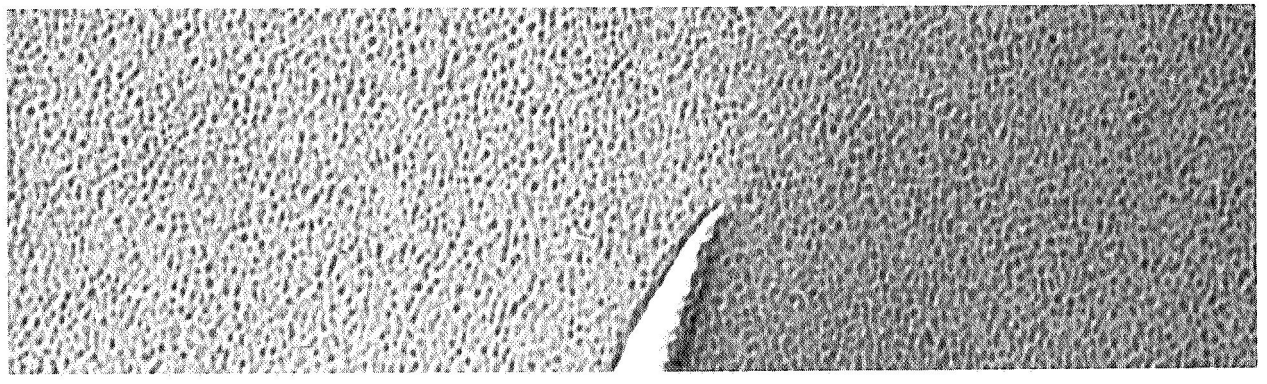

Figure 25. Image After 5 Minute Copper Deposition, Magnification

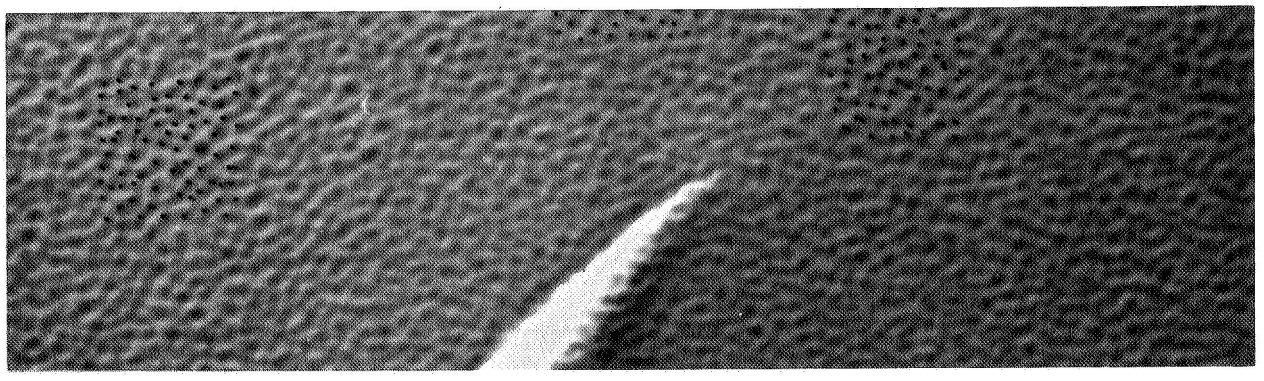

Figure 27. Image After 7.5 Minute Copper Deposition, Magnification 1 : 192,000.

between them diminished and the particle contours became more distinct. The shape of the particles deviated noticeably from the formerly circular habit.

At this state of deposition, distinct crystallinity of some of the larger particles became evident by their deep contrasts of "Bragg reflections" (Reference 19). In the diffraction rings (Figure 29) taken 11.5 minutes after the start of deposition, they appeared as bright spots producing a granulated appearance. At this time the largest crystallites were measured to have dimensions of up to 150 Å.

Figure 29, represented exposure number 18 in this experimental run and at this point, i.e., approximately 11.5 minutes after start of deposition, the run was interrupted to exchange photographic plates. This takes place in a sealed-off camera. Substrate heater current, environmental cooling and electron beam intensity were kept constant during the interruption and the evaporation beam was intercepted by the crystal oscillator and checked. The camera was fully prepumped before it was reopened to the microscope column. The background vacuum gauge at the camera showed a momentary pressure increase from 1.5×10^{-5} to about 2.5×10^{-5} torr for about 20 seconds.

When observation was resumed, i.e., after deposition pause of about 7 minutes, the appearance of the deposit had changed (Figure 30). Before new material was added, the copper crystallites had grown to approximately double their former diameters and had distinct surfaces. Their number per unit area had dropped to approximately one third. The distances between them were wider in many locations. However, due to their irregular shapes many particles nearly touched each other. When copper deposition (with nearly the same rate as before) was continued, the growth mechanism could be observed to be distinctly different from the one before the interruption (Figures 30, 31, 32, 33, 34). Cofluence of crystallites was the dominating process with the resulting defect structures remaining in the crystals. The changes in the shape and size of the crystallites took place without noticeable motions of the combining particles. The location even of the smaller crystallites seemed to be remarkably stable. The diffraction patterns established during the same deposition period conform to the image observations. The granulation in the diffraction rings coarsened approximately with the increasing size of the crystallites (Figures 35, 36).

After a second period of 15 minutes deposition (i.e., approximately 33.5 min after initial start of deposition), the film had grown to cover approximately 90% of the surface, the optical thickness by interferometer measurement was found to be between 200 and 300 Å. After a final observation, the deposition was stopped at this point and the substrate heater turned off. The temperature of the substrate dropped to temperatures below room temperature within a few minutes. When the cooled deposit was hit by the electron beam, crystals combined with dramatic

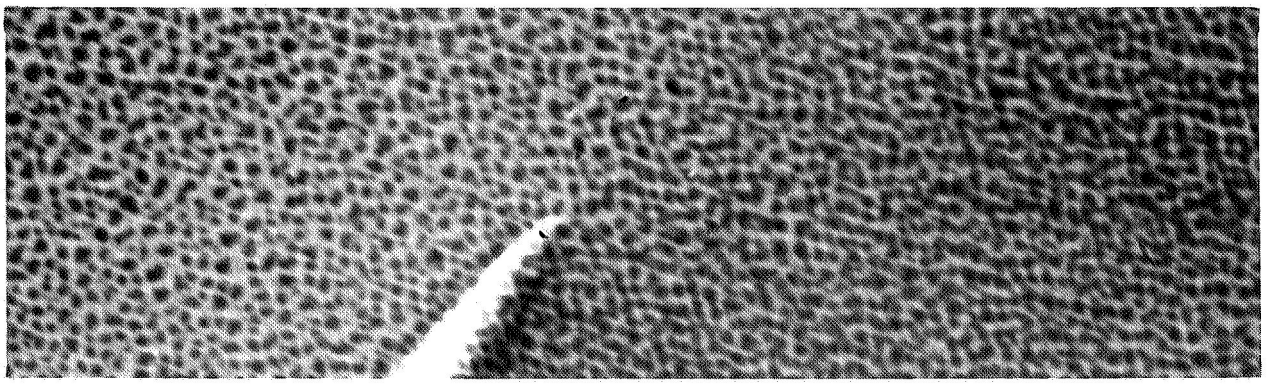

Figure 28. Image After 11 Minute Copper Deposition, Magnification 1 : 170,000.

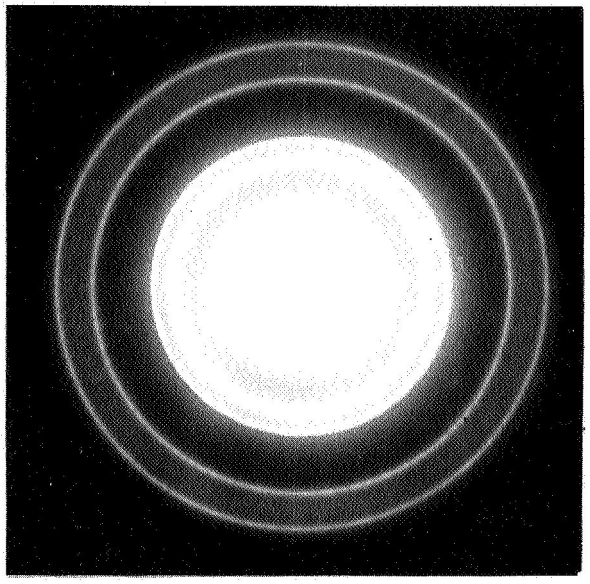

Figure 29. Diffraction After 11.5 Minute Copper Deposition (Image Figure 28).

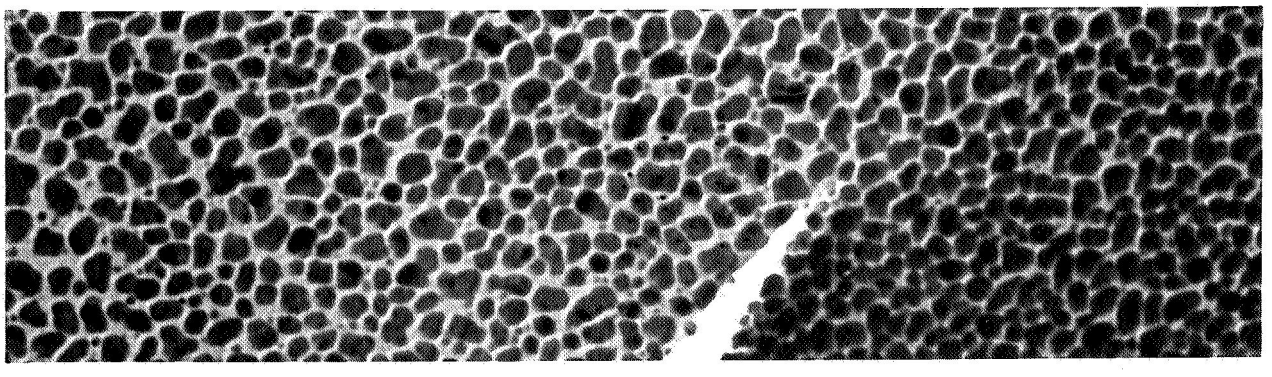

Figure 30. Image After 18.5 Minute Copper Deposition, Magnification 1 : 170,000.

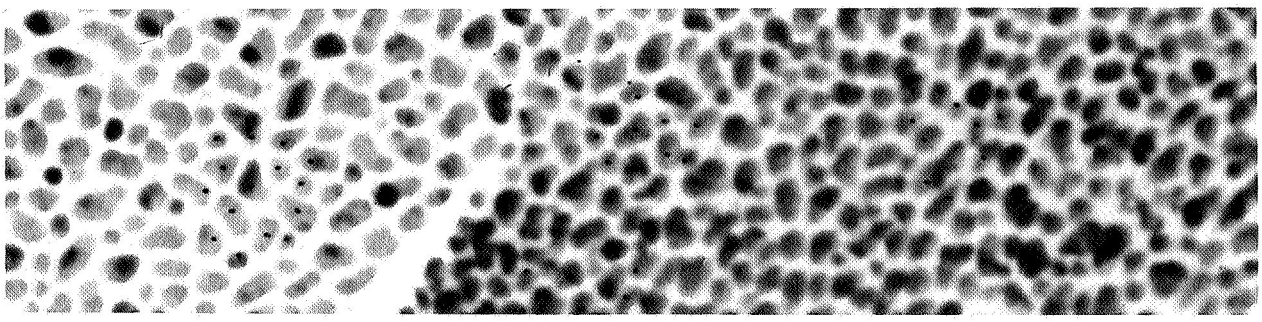

Figure 31. Image After 21.5 Minute Copper Deposition, Magnification 1 : 170,000.

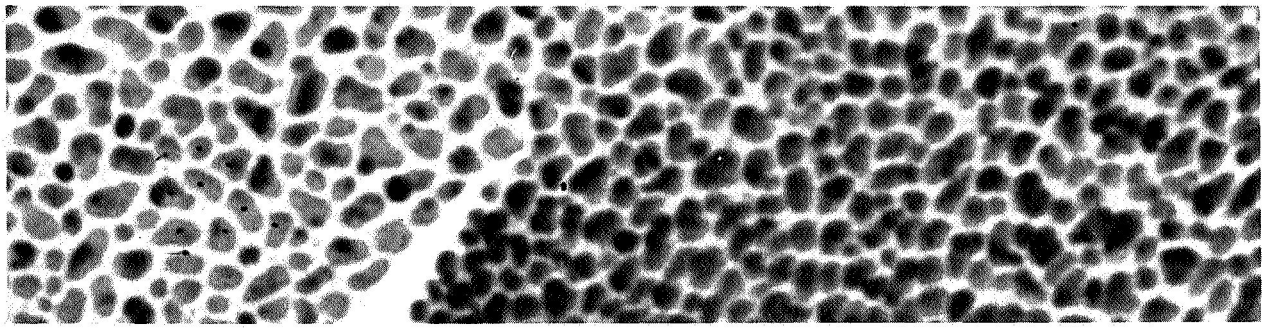

Figure 32. Image After 21.75 Minute Copper Deposition, Magnification 1 : 170,000.

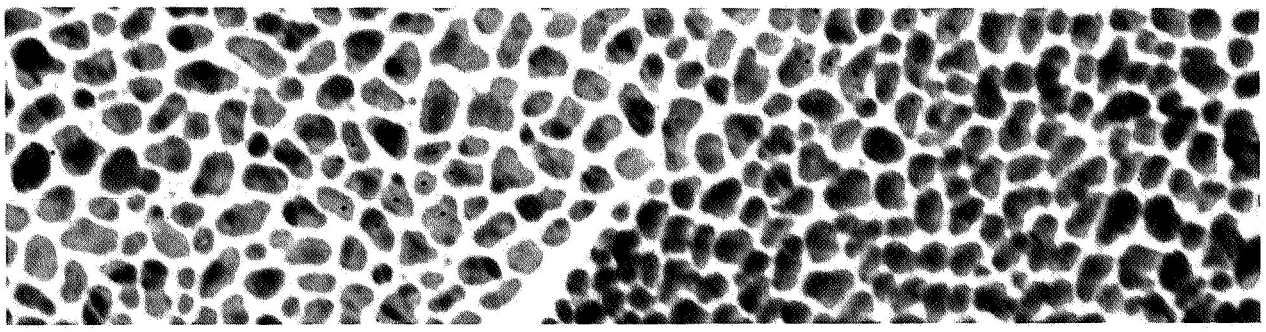

Figure 33. Image After 23.5 Minute Copper Deposition, Magnification 1 : 170,000.

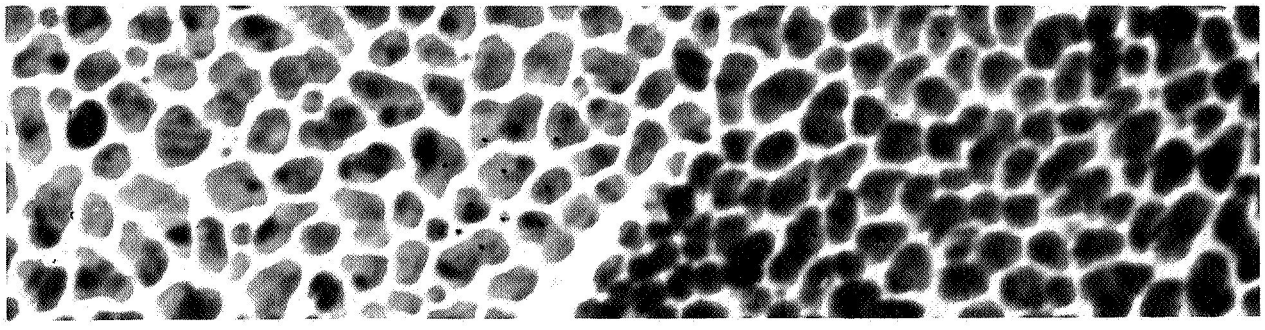

Figure 34. Image After 29.5 Minute Copper Deposition, Magnification 1 : 170,000.

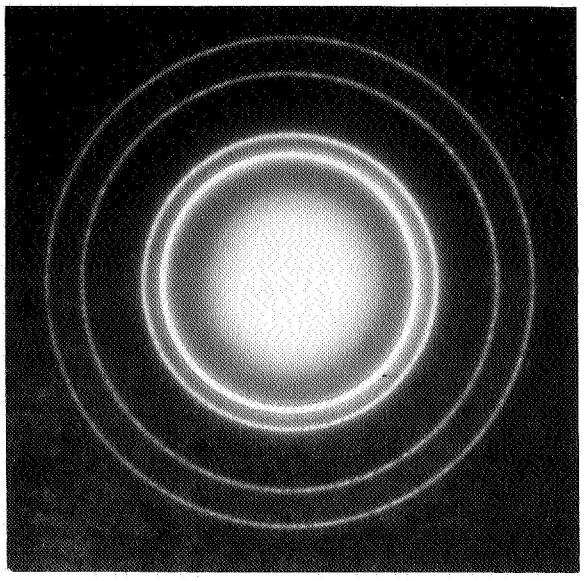

Figure 35. Diffraction After 19.5 Minute Copper Deposition (Image Figure 30).

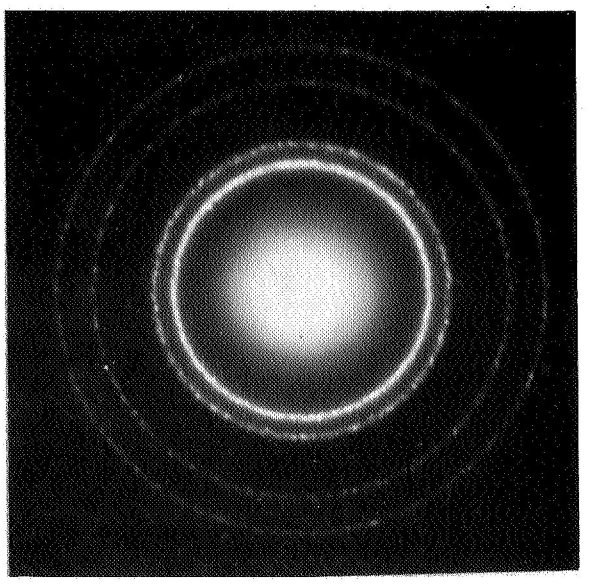

Figure 36. Diffraction After 28 Minute Copper Deposition (Image Figure 34).

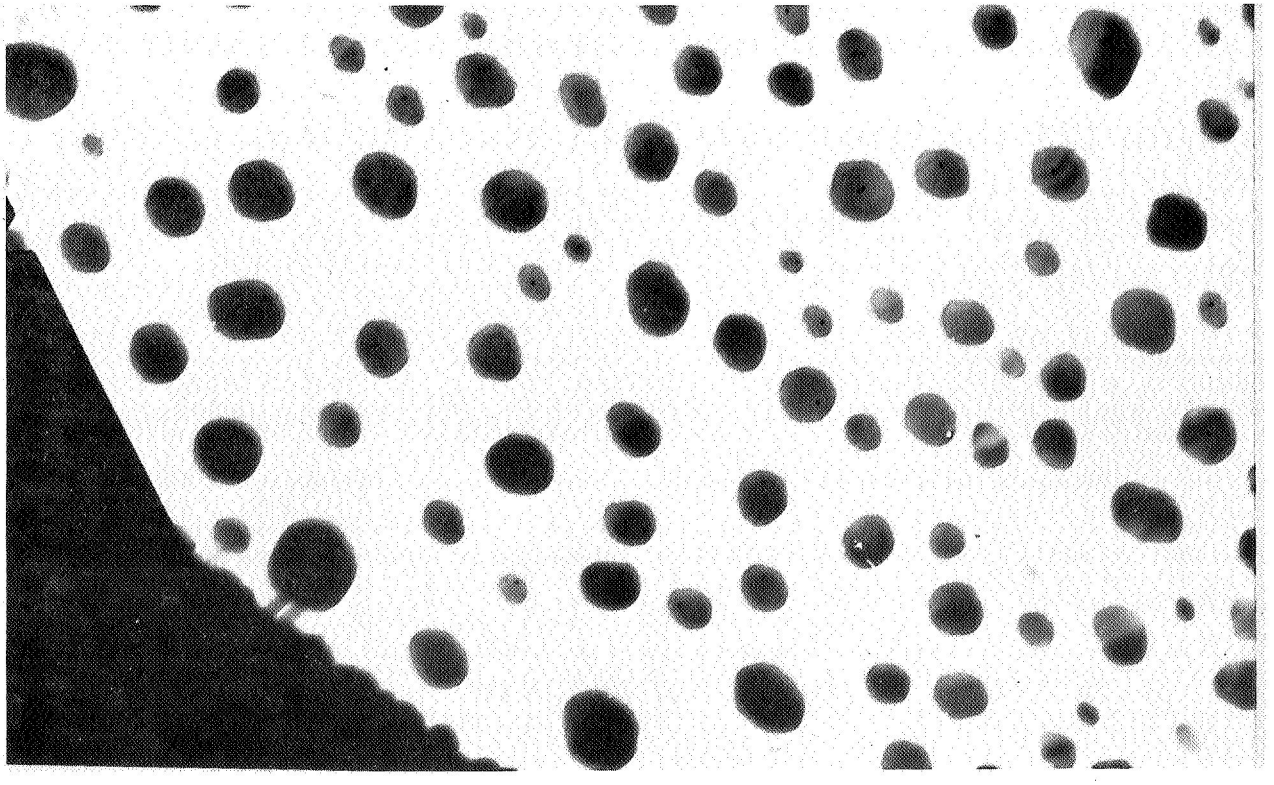

Figure 37. Image of Globular Copper Particles Formed on Carbon After Cooling (Diffraction Figure 38).

suddeness. Within seconds - defying efforts to obtain photographic records - the irregular crystalline particles became globular in shape moving over distances of microns and combining to globules of 500 Å diameter or more (Figure 37). The corresponding diffraction pattern showed diffraction rings composed of separated irregular diffraction dots and included carbon diffraction of substantial intensity (Figure 38). The diffraction shows that the entire copper deposit had coagulated into crystals with spherical contours of diameters from 500 Å to several thousand angstroms, distributed fairly evenly on an otherwise clean carbon substrate.

Copper Growth Under Room Temperature Conditions. - During the deposition of copper on carbon at room temperature, carried out at low deposition rates, progressive initial nucleation was again evident by the growing number of diffraction rings. Contrast enhancement of the carbon surface became obvious at very early states of the deposition. The first visible coagulation of the deposit occurred in the form of widely separated particles of about 50 Å - 60 Å size (Figure 34). Bragg reflections within these crystallites were not observed. After 6 more minutes deposition time, most particles were larger than 80 Å (Figure 40). Many of these produced a high-contrast image and a thoroughly crystalline diffraction ring system. Further deposition did not change the basic appearance of such a film.

For qualitiative comparison, a fast, room temperature deposition of copper on fresh carbon was carried out in a high vacuum system (10^{-6} to 10^{-7} torr background pressure). Due to uncertainties in relative substrate temperatures and deposition rates, this singular experiment is insufficient for reaching any conclusions and is presented here only for completeness of reporting. Figures 41 and 42 typify the results. There is a considerable dissimilarity in shape, size distribution and density. Reasons for this can only be evaluated when the deposition parameter control in the insitu unit is updated by the recently developed techniques. As can be seen from the figures, most of the deposited material consisted of circularly shaped copper particles of diameters from 100 to 300 Å. Defect structure contrast and diffraction ring systems showed well established crystallinity and the visibility of the two diffuse diffraction rings of amorphous carbon proves the presence of a substantial area of empty carbon substrate.

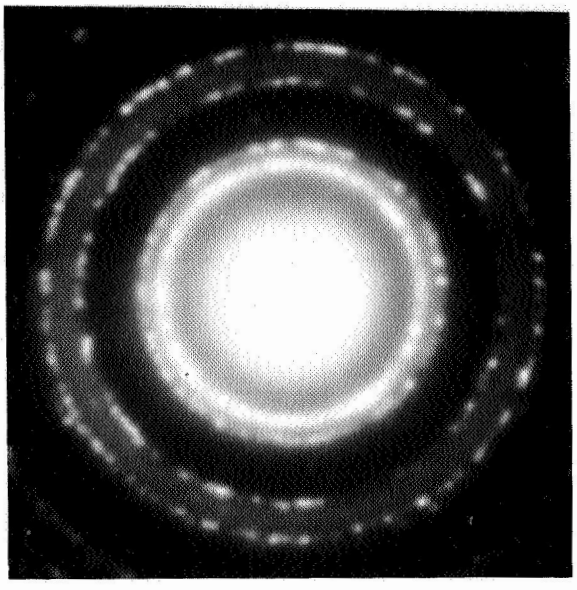

Figure 38. Diffraction After Formation of Globular Copper Particles (Image Figure 37).

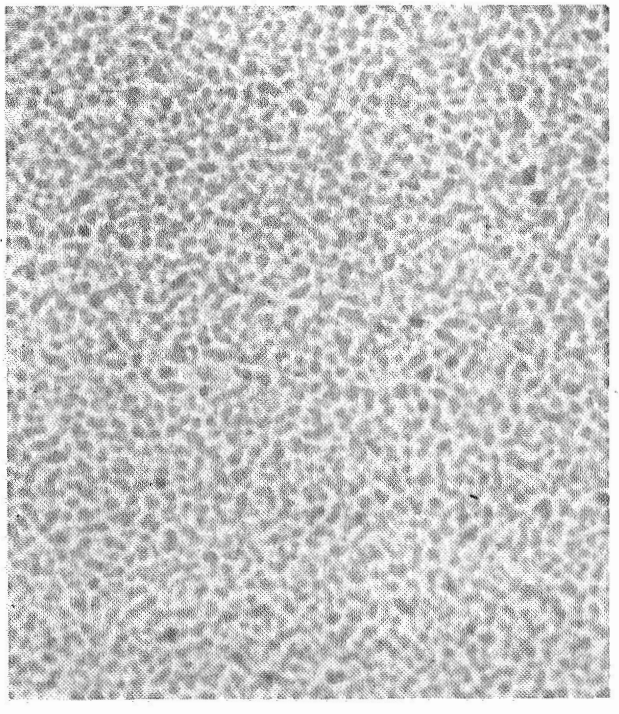

Figure 39. Image of Copper Deposition After 47 Minutes at Room Temperature Magnification 1 : 144,000.

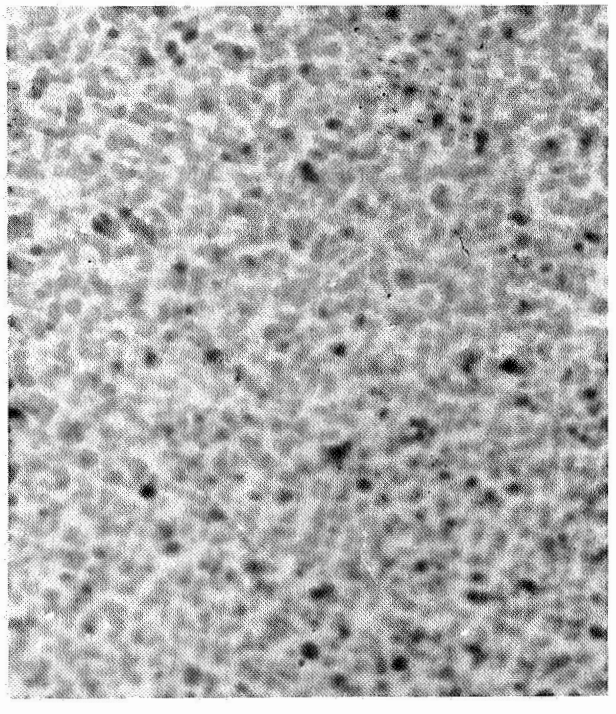

Figure 40. Image of Copper Deposition After 53 Minutes at Room Temperature Magnification 1 : 144,000.

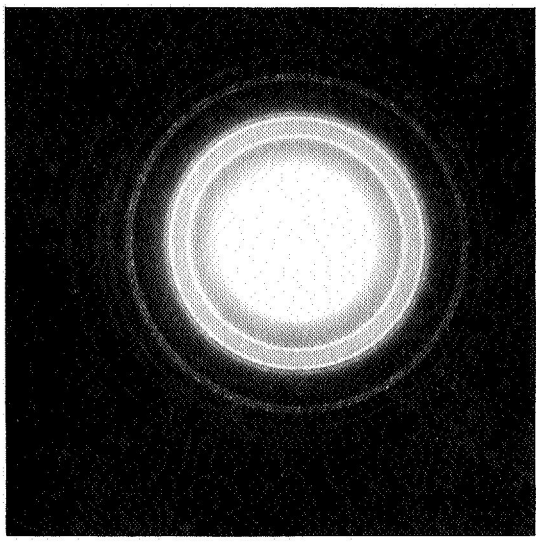

Figure 41. Diffraction of Spherical Copper Particles (Image Figure 42).

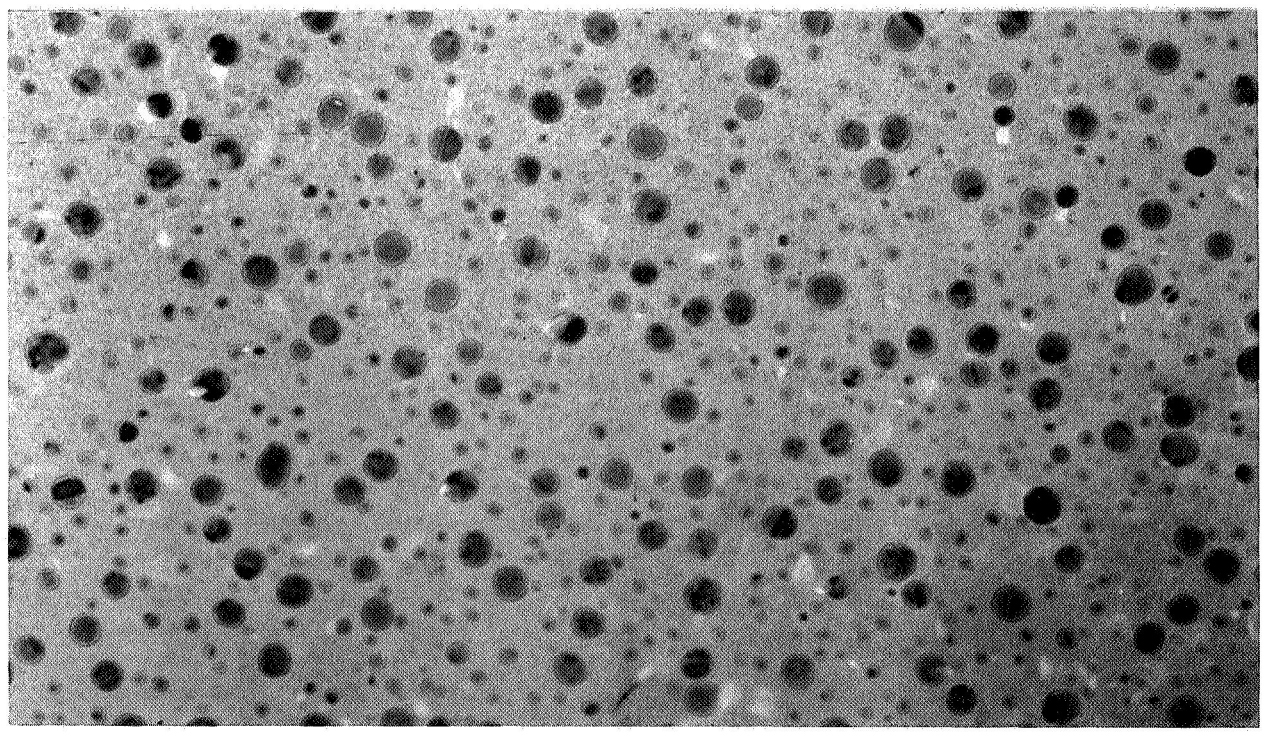

Figure 42. Image of Spherical Copper Particles at Room Temperature Defocussed for Defect Contrasts, Magnification 1 : 200,000.

Gold Deposition At Room Temperature

Gold is known to coagulate at very early stages of deposition. For this reason, it is not useful as a shadowgraphing material for high-resolving electron microscopy. The granulation into small (20 Å) contrast rich particles is often utilized for resolving power tests of electron microscopes.

The in-situ gold depositions were carried out using a 99,999% pure gold source and a fresh carbon substrate heated to room temperature against the liquid nitrogen cooled environment. Under these conditions, early conglomeration was not observed in gold deposits. 5 minutes after the initiation of deposition, nucleation became evident by the inner (111) diffraction ring of gold appearing inside the diffuse diffraction ring from the carbon. It took 4 more minutes of deposition time until electron images gave some evidence of deposition (Figure 43). At this time, the diffraction pattern consisted of 5 distinct rings plus the two rings of amorphous carbon which were still in evidence (Figure 44). The images during several minutes of continued deposition showed the surface structure of the carbon film with increasing contrast. Details from 10 Å up were recognizable, and no particle coagulation was observed up to about 16 minutes of deposition time (Figure 45). During the next 2 minutes of deposit, coagulation did occur as well as changes in the growth habit of the deposits. The diffraction rings of the gold narrowed down to a fraction of their former width and the diffuse rings of the carbon substrate appeared stronger again. In the image the structural features of the carbon surface cannot be seen anymore, however, the deposited material forms many particles of 50 Å and larger which are found in surroundings of lighter areas apparently indicative of denuded carbon (Figures 46, 47). After the exposure leading to Figure 47, film plates were exchanged. In contrast with the earlier observations on copper, the deposit was found unchanged immediately after exchange of photographic plates (Figure 48). But, the electron beam used for the observation seemed to have an effect on the deposited particles. Within one minute of observation, the image changed by a sudden coagulation activity. Without additional depositions particles combined to form crystallites with sharp contours and irregular shapes (Figure 49). Particle size average had increased from about 100 Å to 200 Å.

Keeping this area of the sample under the effect of the observation beam while resuming deposition did not result in significant further growth of the established particles. The existing particles stayed in place and the entire arrangement, gold particles and the open carbon areas, served as a substrate for a new deposition. New particles could be recognized over the carbon substrate as well as on the formerly deposited particles (Figure 50). In this figure the new particles have an average diameter of 50 Å.

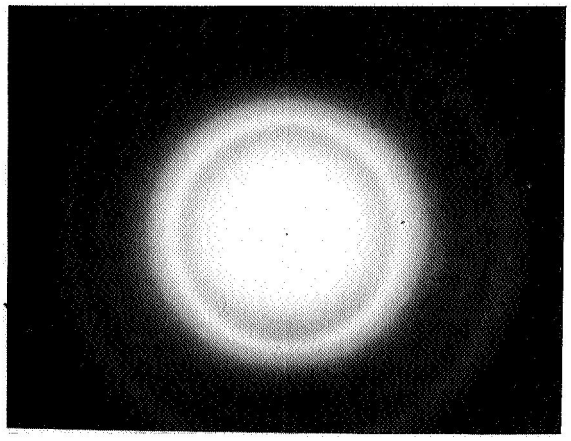

Figure 43. Diffraction of Gold Deposition After 9 Minutes.

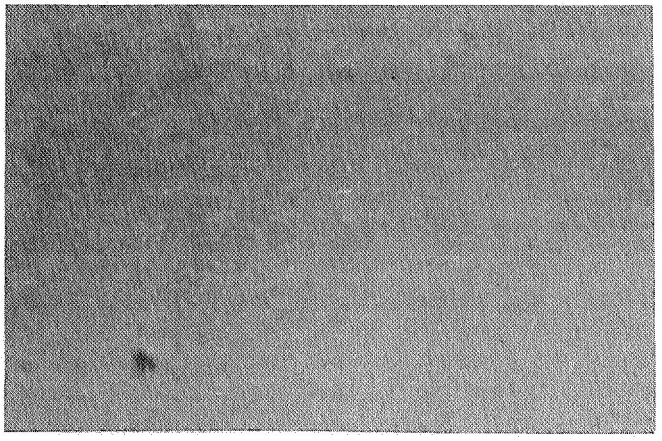

Figure 44. Image of Gold Deposition After 9.5 Minutes, Magnification 1 : 94,000.

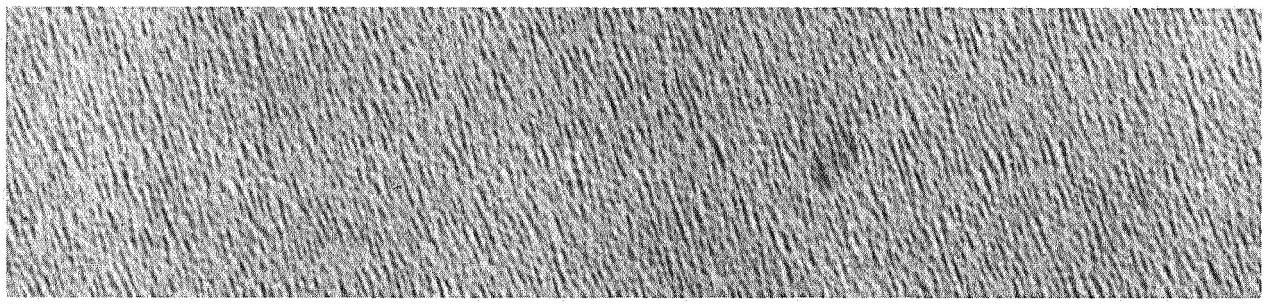

Figure 45. Image of Carbon After 16 Minute Gold Deposition, Magnification 1 : 94,000.

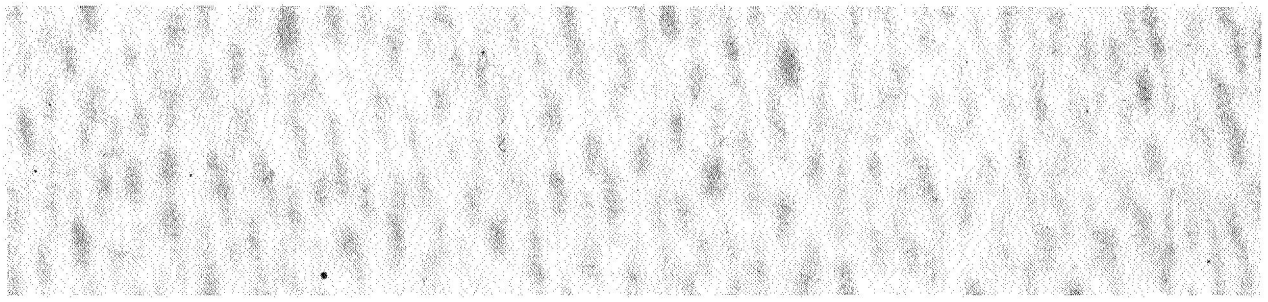

Figure 46. Image After 20 Minute Gold Deposition, Magnification 1 : 364,000.

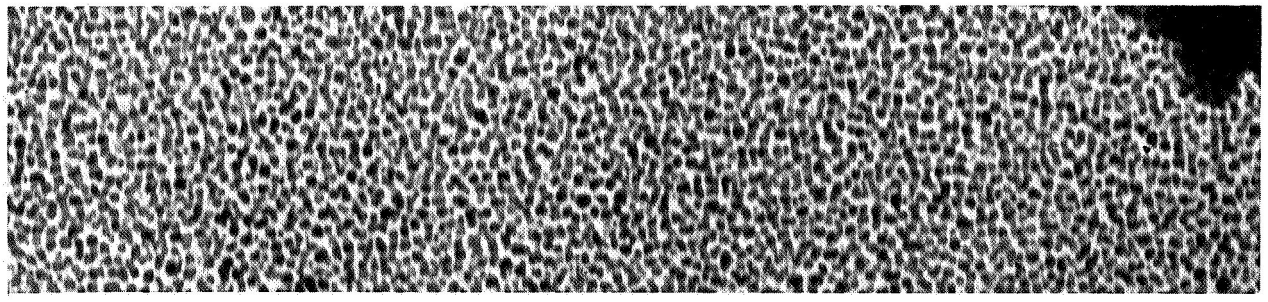

Figure 47. Image After 33 Minute Gold Deposition, Magnification 1 : 120,000.

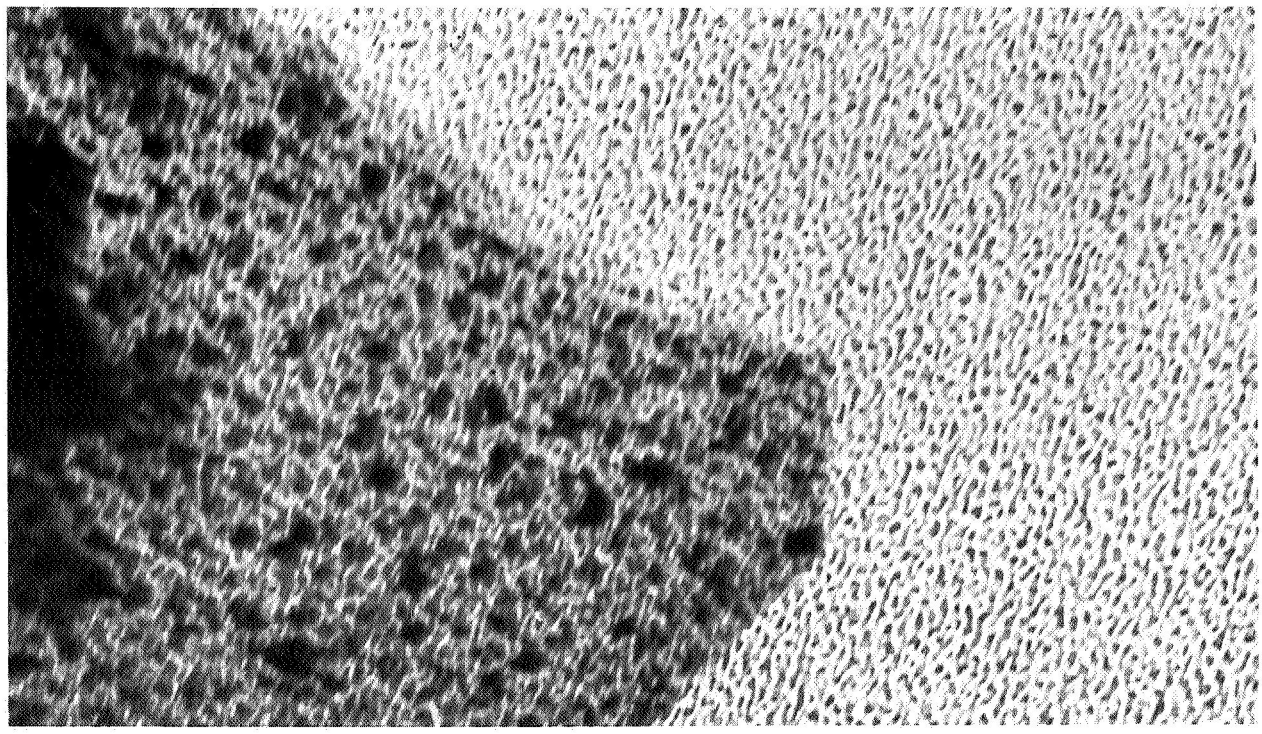

Figure 48. Image After 33 Minute Gold Deposition After Interruption for Change of Photographic Plates, Magnification 1 : 120,000.

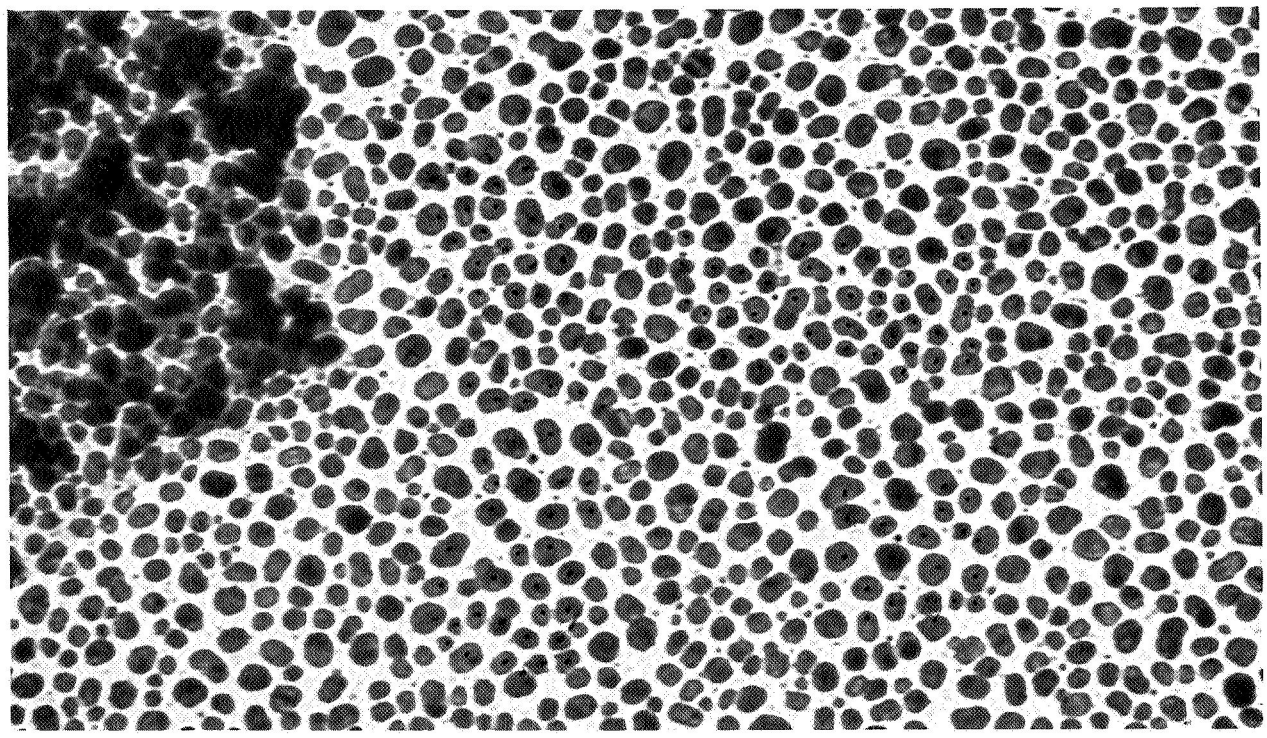

Figure 49. Image After 33 Minute Gold Deposition After 1 Minute Exposure to Electron Beam, Magnification 1 : 192,000.

The effect of extented exposure to the observation electron beam in this sequence of depositions can be seen by comparison with areas of the deposited film which were not exposed to the electron beam after plate exchange. Such areas (Figure 51) were found nearly covered with deposited gold particles of complex shapes. They appeared to be essentially flat and showed a well developed crystallinity as is evident from the diffraction pattern (Figure 52).

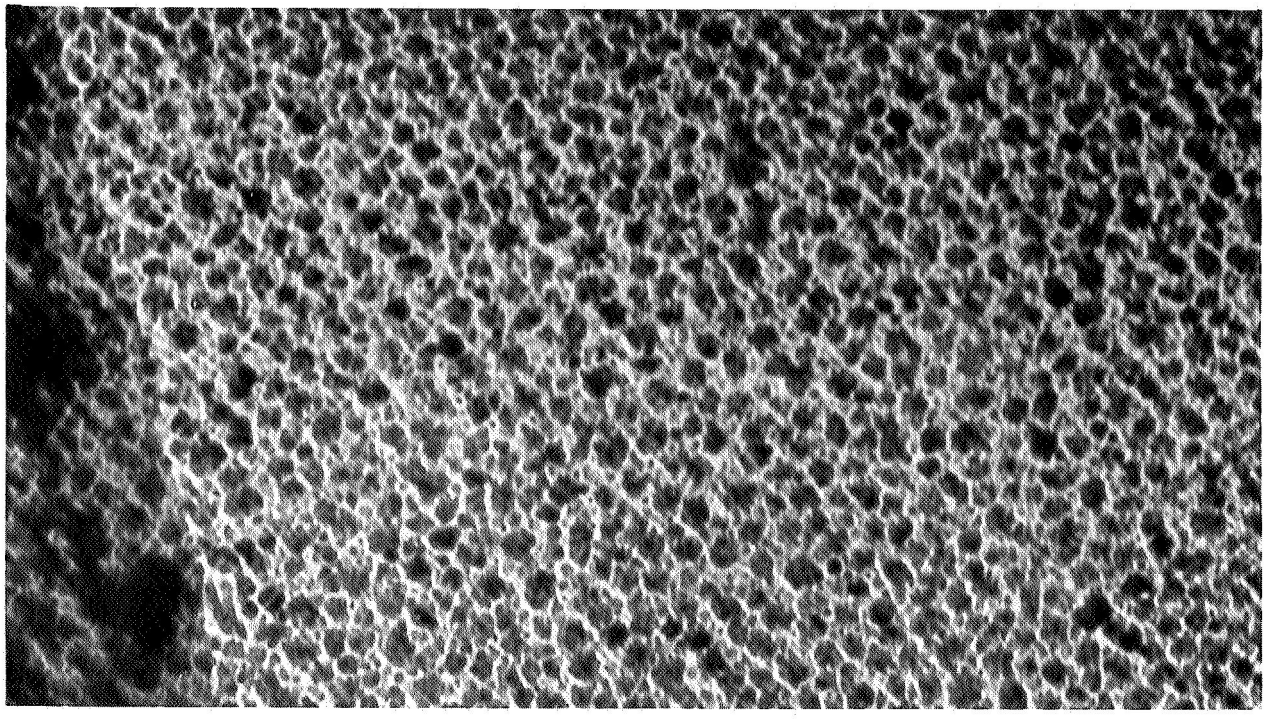

Figure 50. Image After 75 Minute Gold Deposition on Formerly Observed Location, Magnification 1 : 192,000.

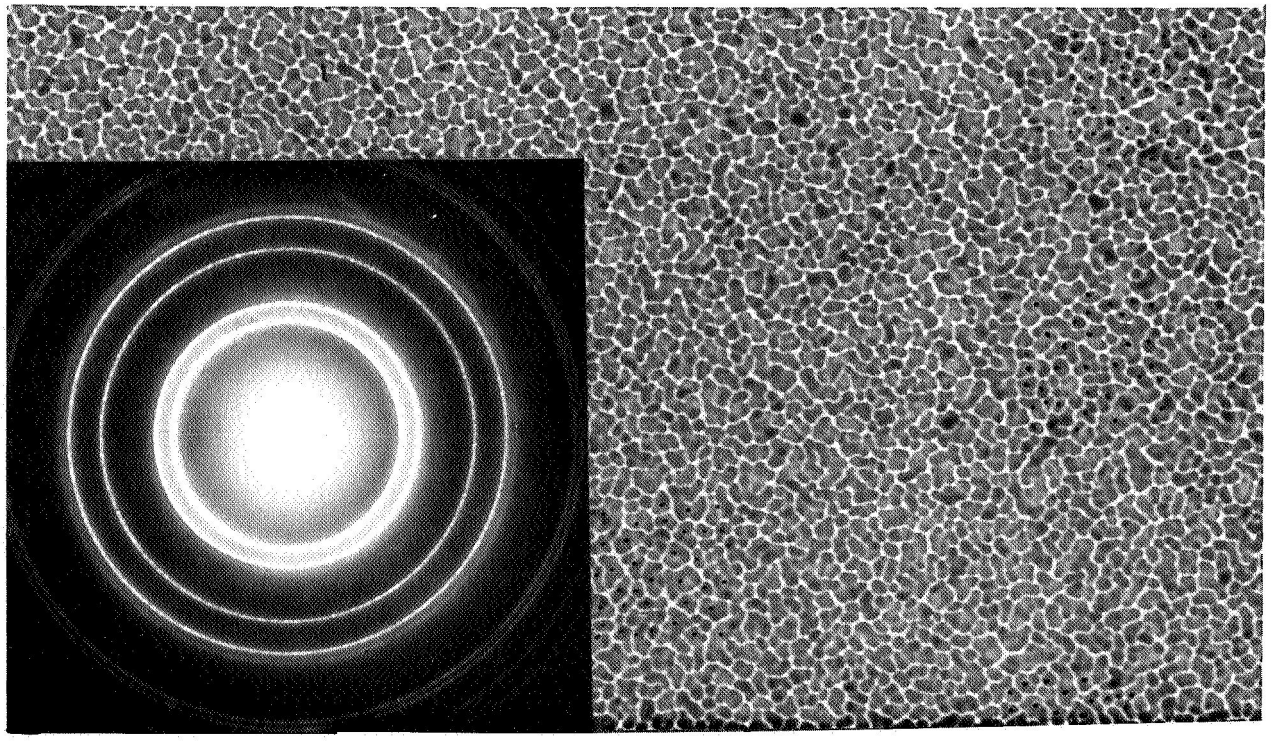

Figure 52. Diffraction After 75 Minute Gold Deposition.

Figure 51. Image After 75 Minute Gold Deposition on Location Without Former Observation, Magnification 1 : 192,000.

DISCUSSION OF RESULTS

The Formation of Crystallites. - One of the objective of these studies has been the detection of significant changes of crystallinity during early stages of film deposition. At all temperatures investigated, the deposition of iron, copper and gold started in a shadowgraphing fashion governed by the incident angle of the deposits and the surface undulations of the pure amorphous carbon which was always used as a substrate. No particular crystal habits prevailed. The depositing material accumulated at the ridges of less than 20 Å size which formed the general undulation of the surface of evaporated carbon layers. If the deposited material was composed of separated nuclei at this stage, they must have been smaller than the resolving power of the microscope (approximately 15 Å). Before the deposited material produced a noticeable contrast in the electron image, its presence manifested itself in the appearance of at least one diffraction ring, in all cases the (111)-ring of a face centered cubic lattice.

C.W.B. Grigson and E. Barton (Ref. 17) have investigated the Debye intereference function for small units of face centered cubic lattices. Crystallites composed of 27 to 55 atoms will not produce more than 3 diffraction rings (111, 220, and 311). The appearance of the (200)-ring indicates the presence of crystallites containing more than 64 atoms. The innermost ring may be visible when 4 atoms start to maintain distances of the appropriate crystal lattice.

Assuming those theoretical developments to be applicable in our case, our deposits in the early stages were composed of quasi-amorphous metal containing many small groups of 4 to 8 atoms forming crystallites of sizes equivalent to their lattice parameter.

In most of our experiments about 4 diffraction rings could be identified, before the image of the deposit changed significantly.

Further deposition of copper or gold did not proceed in the form of continuous growth and monotonously higher substrate over-growth. Within the exposure time of one or two micrographs, we found particles which had grown considerably faster by apparently depleting their vicinity of deposited material. All of our experiments yielded measurable images and diffraction patterns. A prevailing particle size of about 80 Å was evident when the first sharp, well developed diffraction rings were produced.

Liquid Phase

At the temperature applied in our experiments, no "liquid" phase has been identified in any of the deposits. Even deposits which had a well rounded shape and which appeared to have a high mobility shape (Figures 37, 41) could always be identified to be crystalline in nature by diffraction and by observed defect structures which were clearly visible in slightly defocussed images. This general appearance of well established crystallinity may not exclude - however, the existence of an amorphous surface layer with quasi liquid behavior which could not be resolved by the instrument.

Transformation of Crystal Lattice Type

Only in iron did we observe a transformation of one crystal lattice type into another. Face centered cubic crystallites could be observed and by diffraction rings. Sizes of f.c.c. crystallites were limited to 30 Å at room temperature, and 50 Å at elevated temperatures. The observed f.c.c. diffraction ring systems transformed into a different diffraction system before becoming sufficiently sharp for accurate measurements. The f.c.c. (111) ring became gradually fainter while new rings appeared. An intense and sharp ring, indexed as (200) in a body centered cubic lattice coincided with the more diffuse ring which was indexed as (220) in the face centered cubic lattice.

When this transformation occurred at elevated temperatures, it resulted in a completely b.c.c. iron deposit. We also have found the two crystal types in close proximity to each other, (Figure 15). Also an intermediate situation has been found stable enough to be studied (Figure 16). A more definite and detailed analysis of the transition of the f.c.c. iron cyrstallites into larger b.c.c. iron crystallites should be based on larger experimental sampling.

Change in Lattice Parameters

Neither in copper nor in gold did we find any changes in lattice parameters. From the start of the appearance of the innermost ring, no systematic changes in the lattice parameters of the crystallites were measureable during the deposition. Differences in ring diameters were not systematic and were always consistent with changes in the instrument constant $L\lambda$, which was checked before and after each experiment by diffraction patterns of fully developed and identified films.

In the observations of iron deposits, by contrast, we found an enlarging of the ring diameters with growth. The changes were small and consistent but accuracy of their measurements are limited by the very diffuse nature of the initial diffraction pattern.

Particles of less than 50 Å size possessed a f.c.c. cell edge of about 4.3 to 4.2 Å. In the 50 Å range - and during crystal type transformations, the b.c.c. rings indicated lattice dimensions of approximately 3.1 Å. Such particles, observed as they grew to about 100 Å size, changed to a lattice parameter of about 2.90 Å.

The Growth Habit of b.c.c. Iron Particles

The growth of b.c.c. iron particles did not proceed in the same manner as observed for other metals. All the iron films which we produced showed a strong preference for formation of crystals in straight rows of up to 30 particles of approximately 30 Å diameter each. Such rows have been observed parallel to each other or in perpendicular arrangements. Row formations were also observed as substructures when the deposit covered large areas of the substrates. By through-focus series of observations, which revealed crystal habits independent from focussing effects or from photographic grain effects, the row structure of b.c.c. iron films was consistently found as long as the environmental conditions provided high purity source material. This was also found to be independent of the carbon surface conditions. The deposit did not grow differently on a pure carbon film than it did if the carbon was covered by a silicon monoxide layer.

We suggest as one possible explanation of the observed growth characteristics that on transformation of the initial crystallites into b.c.c. iron renders the particles increasingly ferromagnetic. A consequent long range interaction effect on the arrangement of the neighboring deposit into parallel and/or anti-parallel magnetic dipole orientations seems then quite feasible.

A possible analogy exists in bulk nucleation processes used for precipitation hardening of certain, solid ferromagnetic materials without or with magnetic field (Ref. 20, 21). Elongated particles grow either in the direction of the spontaneous magnetization or in the direction of an outer field which is used to make the magnetization of all nuclei unidirectional. This magnetically preferred nucleation and crystallite growth inside solid state crystalsrequires undisturbed conditions (free from carbon impurities or strains). Therefore, impurity effects are likely to influence the preferential growth mechanism in iron films also. This deserves consideration in future work.

Iron "particles" in liquid form are also known to nucleate and grow along the lines of their magnetization (Ref. 22, 23) provided all other nucleation effects, even mechanical motion, are excluded. This ferromagnetic films can be produced with magnetic anisotropies when they grow under the influence of a magnetic field (Ref. 24).

The particular shapes of the b.c.c. iron cyrstallites prevented the coordination of the observed effects to defined particle sizes. In order to deposit iron with a defined particle size a higher temperature should be applied, close to or above 770°C (Curie point). The effect of magnetic poles on nucleation and growth would then not interfere with the formation of crystals with a regular habit.

Particle Growth and Environmental Conditions

Four different types of growth processes have been observed during insitu deposition:

1) Adsorption and growth of deposited metal on the carbon surface with some apparent influence of material.

2) Island formation of deposited material.

3) Cofluence of adjacent islands into particles with sharp contours.

4) Combination of particles over relatively large distances.

The first process produced a gradual contrast increase of the image of the carbon surface. The deposited material did not show any preferential habits within the resolving power of the instrument (15 Å).

The second process resulted in random or preferential (b.c.c. iron) arrangements of particles from 30 to 50 Å size located within areas of apparently denuded carbon. The image of the deposit did not show the relation to the carbon surface structure which had been in evidence during the first process.

The first two processes have been observed under clean and undisturbed conditions for all metal depositions carried out.

The third and fourth process have been observed in our experiments only after an interruption of the in-situ experiments, the possible introduction of contamination or after conclusion of the deposition and cooling. A quasi-liquid like behavior (high mobility, round shape) could be noted occassionally, though all particles showed crystalline structures throughout.

The cofluence process took place between particles in close proximity to each other, without extensive lateral motion. The crystal orientation of the formerly separated particles could usually be recognized inside the particle which resulted from the combination. Thus, in effect this process is mostly a growing together, rather than a cofluence in the sense, of liquid droplets. The particles appeared to be flat compared with their lateral extension. The observation beam seemed to have some effect on the process as comparisons had shown between locations under long and short observations.

The fourth process was observed to be initiated by the electron beam of the instrument. The particles assumed near globular shapes without loosing their crystallinity. They were seen moving over longer distances, often propelled to considerable velocity suggesting effects of surface charges.

The sensitivity of deposits, nucleated and grown under clean conditions, to changes of their environmental conditions should be studied further. The observation of the different growth phenomena and their relation to environmental conditions, if not fortuitous, may become an important side result of these studies.

REFERENCES

1) L. Bachmann and H. Hilbrand, Proc. Int. Symp. Clausthal-Goettingen 1965, p. 77-82.

2) J. W. Matthews, Vac. Sci. Techn. 3, 1966, 130.

3) E. Bauer, A. K. Green, K. M. Kunz, H. Poppa, Proc. Int. Symp. 1965 Clausthal-Goettingen, p. 135 - 152.

4) T. A. McLauchlan, R. S. Sennett, G. D. Scott, J. Appl. Phys. 21, 1950, 72.

5) G. A. Bassett, Proc. Europ. Reg. Conf. El. Micr. Delpht 1960, 270.

6) D. W. Pashley and M. J. Stowell, 5th Int. Conf. El. Micr. 1962 Philadelphia GG1.

7) H. Poppa, 5th Int. Conf. El. Micr. 1962, Philadelphia GG14.

8) H. Poppa, Trans. 9th Nat. Vac. Symp. McMillan Co. 1963.

9) D. W. Pashley, H. J. Stowell, M. H. Jacobs, and T. J. Law, Phil. Mag. 8th Ser. 10, 1964, 127 J. Vac. Sci. Techn. 3, 1966, 156.

10) H. Poppa, J. Vac. Sc. Techn. 2, 42, 1965 and GDC-ERR-AN-815, December 1965.

11) U. Valdre, D. W. Pashley, E. A. Robinson, M. J. Stowell, K. J. Ruthledge, and R. Vincent, Proc. Int. Conf. El. Micr. Kyoto, 1966, 155.

12) C. W. Grigson, W. C. Nixon, and F. Tothill, Proc. Int. Conf. El. Micr. Kyoto, 1966, 157.

13) H. Poppa, NASA-TN-A-2544, 1967.

14) H. Poppa, J. Appl. Phys. 38, 1967, 3883 - 3894.

15) L. Bachmann and B. M. Siegel, Proc. Europ. Conf. Delpht 1960, 157.

16) R. E. Burge and N. R. Silvester, Proc. Europ. Conf. Delpht 1960, 161.

17) C. W. B. Grigson and E. Barton, Brit. J. Appl. Phys. 18, 1967, 175.

18) D. B. Dove, C. W. B. Grigson and G. R. Stillwell, J. Vac. Sci. Techn. 3, 1966, 120.

19) P. B. Hirsch, A. Howie, M. J. Whelan, Verh. 4th Int. Conf. Berlin 1958, 527.